



بِسْمِ اللّٰهِ الرَّحْمٰنِ الرَّحِیْمِ

Sudan University of Science & Technology
College of Petroleum Engineering & Technology
Exploration Engineering Department

Graduation Project about:

**FORMATION EVALUATION IN HAMRA OIL-FIELD BY USING
WIRELINE LOGS**

تقييم الطبقات في حقل حمرا باستخدام تسجيلات الابار

Submitted to College of Petroleum Engineering & Technology in Sudan University partial fulfillment for one of requirement to take the degree of B.Sc. Exploration Engineering

Prepared by:

1. ABD ALRAHMAN HASSAN ABD ALRAHMAN
2. AHMED HASHIM TAYFOR
3. AMRO ABU ALGASIM ABD ALRAHMAN
4. HUSSAM ALI IBRAHIM MOHAMMED
5. MOHAMMED AL GASIM MOHAMMED ALI

Supervisor:

Eng. AHMED EL NOOR

October, 2017

FORMATION EVALUATION IN HAMRA OIL-FIELD BY USING

WIRELINE LOGS

تقييم الطبقات في حقل حمرا باستخدام تسجيلات الابار

هذا المشروع مقدم إلى كلية هندسة وتكنولوجيا النفط - جامعة السودان للعلوم والتكنولوجيا كإنجاز جزئي لأحد المتطلبات الأساسية لنيل درجة البكالوريوس مرتبة الشرف في هندسة الإستكشاف.

إعداد الطلاب:

1. احمد هاشم طيفور .
2. حسام علي ابراهيم محمد.
3. عبد الرحمن حسن عبد الرحمن .
4. عمرو ابو القاسم عبد الرحمن .
5. محمد القاسم محمد علي .

مشرف المشروع:

• م. احمد النور

التوقيع.....

رئيس قسم هندسة الاستكشاف:

• أ. عبد الله عبد الجبار التوقيع.....

عميد الكلية:

• د. تقوى أحمد موسى

التوقيع.....

التاريخ 12 / 10 / 2016م

Acknowledgement

**It is our great pleasure to have chance in order to say
thank you to our teachers in College of Petroleum
Engineering, Our supervisor:**

ENG. AHMED EL NOOR

Our great thankfulness to:

ENG. AHMED MUSTAFA MABROUK

**We highly appreciate the help of us, for his valuable
comments, encouragements, guidance and support.**

**We would like to thank all our colleagues for their
support and information that helped us to conduct
this research....**

To my dear parents

I can't thank you enough for all the support and sacrifices you have done to me when I needed them. I'm grateful to have both of you by my side; it gave me strength and guidance. I wouldn't have become the man I am today if it wasn't for the both of you. Thank you for believing in me, I promise to never let you down

I love you with all my heart and I'm proud to be yours

To our brothers and sisters

To our friends

To our teachers

Thank

You

all

Abstract

Formation evaluation can be performed in several stages such as during drilling, after logging as detailed log interpretation, and core analysis in the laboratory, etc. This study shows the formation evaluation using wireline log data of hamra oil Field (MH-1). Lithology has been identified from Spectral, Natural Gamma Ray logs and SP where hydrocarbon bearing zones are detected by resistivity and lithology logs including cross checking of porosity logs. The shale volume is estimated from Gamma Ray and True resistivity methods, respectively. Porosity has been estimated from single log methods as well as from Neutron-Density combination formula and Sonic log. Formation water resistivity is estimated from Inverse Archie's, Rwa analysis. The Archie's, Indonesia and model have been used for water saturation estimation. According to log data analysis, there is baring sand zone well where small mud cake is present within oil bearing sand zone depth interval. Lithology is laminated shale and silt. The average gamma ray value and resistivity ranges are 49-102 API and 11-23 ohm-m of reservoir sands. The shale volume is about 20and percent from Natural Gamma Ray and True resistivity methods of thick sand with 14.2 meter reservoir thickness of bantiu. Average formation water resistivity for virgin zone is 0.04 ohm meter. This oil bearing reservoir sand porosity and permeability quality is good. The average water saturation is 0.041 percent using aforementioned model, this water saturation is more reliable for estimating reserve estimation and future reservoir analysis of this formation

التجريد

تقييم الطبقات يتم بواسطة عدد من الخطوات المتتالية اثناء عملية الحفر او بعد الحفر لتفسير الخواص البتروفيزيائية للتكوين تستخدم تسجيلات الابار او العينات الصخرية التي تحلل في المعمل او غيرها من الطرق.

هذه الدراسة تقوم بتقييم الطبقات الواقعه في حوض المجلد في حقل حمرا باستخدام تسجيلات الابار التي تم الحصول عليها من ثلاث ابار وهي:

MH-1, MH-2 and MH-4

لتفسير الخواص الصخرية استخدمت تسجيلات اشعه قاما و تسجيل الجهد الذاتي للتكوين الذي من المحتمل ان يوجد به هيدروكربون.

استخدم تسجيل المقاومة النوعيه مع اشعة قاما لمعرفة كمية الطين الموجوده في تكوين الرمل, وجد ان هنالك بعض الصخور المصاحبه لرمل وهي الطين والسلت.

تم استخدام تقاطع تسجيل النيوترون مع الكثافة, والمقاومة الصوتية لتقييم مسامية الصخر, ولمعرفة مياه التكوين استخدم قانون ارشي مع معادله اندونسيا ووجد ان تشبع الصخر في التكوين يتراوح ما بين

(0.023 - 0.04).

متوسط تسجيل اشعة قاما ما بين (102 - 49) API, والمقاومه النوعية للطبقات تتراوح ما بين 2.03 الي 24 ohm.m و السمك في الدراسة (14.2m) في تكوين بانتيو.

درجه تشبع الصخر بمياة التكوين حقيقية لدرجه انها معقوله جدا حيث انها تساوي 0.41.

| TITLE | PAGE |
|---|------|
| CHAPTER ONE INTRODUCTION | |
| 1.1 introduction | 1 |
| 1.2 Objectives of study | 2 |
| 1.3 Methodology | 2 |
| 1.3.1 Lithology identification and hydrocarbon bring zone | 2 |
| 1.3.2 Estimation of shale volume and reservoir thickness | 2 |
| 1.3.3 Assessment of porosity | 2 |
| 1.3.4 Geothermal gradient and formation temperature | 2 |
| 1.3.5 Formation water saturation | 3 |
| 1.3.6 Determine of water saturation | 3 |
| 1.3.7 Moveable hydrocarbon index and bulk volume water | 3 |
| 1.3.8 Log derived permeability | 3 |
| OVERVIEW ABOUT MH OIL FIELD | 5 |
| 1.4 location of study area | 5 |
| 1.5 Accessibility | 5 |
| 1.6 Topography | 6 |
| 1.7 Drainage | 6 |
| CHAPTER TWO THE LITERTURE REVIEW | |
| 2.1 historical background of oil and gas exploration in Sudan | 11 |
| CAPTER THREE METHODOLOGY AND METHOD INVESTIGATION | |
| 3.1 Theory of Well Logs and Formation Evaluation | 16 |
| 3.1.1 Lithology logs | 16 |
| 3.1.2 Porosity logs | 19 |
| 3.1.3 Neutron log | 20 |
| 3.1.4 Density logs | 21 |
| 3.1.5 Sonic Logs | 22 |
| 3.1.6 Resistivity Logs | 23 |
| 3.1.7 Geothermal gradient and Formation temperature | 27 |
| 3.1.8 Formation water resistivity | 27 |
| 3.1.9 Movable hydrocarbon index | 28 |
| 3.1.10 Bulk volume water | 28 |
| CHAPTER FOUR RESULTS AND DISCUSSIONS | |

| | | |
|---------------------------------|---|----|
| 4.1 | Lithology and Hydrocarbon Bearing Zones | 30 |
| 4.2 | Estimation of Shale Volume and Reservoir | 34 |
| 4.3 | Assessment of Porosity | 35 |
| 4.4 | Geothermal Gradient and Formation Temperature | 37 |
| 4.5 | Formation Water Resistivity | 37 |
| 4.6 | Determination of Water Saturation | 38 |
| 4.7 | Moveable Hydrocarbon Index and Bulk Volume Water | 39 |
| 4.8 | Log Derived Permeability | 39 |
| 4.9 | Comparison of Petrophysical Properties with Different Studies | 40 |
| 4.10 | Justification and Uncertainty of the Results | 41 |
| CAPTER FIVE | | |
| CONCLUSIONS AND RECOMMENDATIONS | | |
| 5.1 | Conclusions | 44 |
| 5.2 | Recommendations | 45 |
| 5.3 | Reference | 46 |
| APPENDIX | | 48 |

LIST OF TABLES

| TABLE | PAGE |
|--|------|
| 3.1 petro physical properties of common clay minerals | 17 |
| 3.2:Estimate porosity quality | 19 |
| 4.1 Available log data of MH-2 . | 30 |
| 4.2 Logging Parameter of MH-2 | 31 |
| 4.3 Estimated shale volume using spectral, natural GR. | 34 |
| 4.3 Estimated shale volume using spectral, natural GR. | 36 |
| 4.4 Estimated porosity from sonic log. | 38 |
| 4.5 Estimated Resistivity water saturation from different models. | 38 |
| 4.6 Estimated water saturation from different models. | 40 |
| 4.9 Comparison of Petrophysical Properties with Different Studies. | 48 |
| E-1 Estimation Lithology for MH -4Well | 48 |
| E-2 Assessment porosity from Density Log for MH-4 Well | 48 |
| E-3 Assessment porosity from sonic Log for MH-4 Well | 48 |
| E-4 Assessment porosity from Neutron Log for MH-4 Well | 49 |
| E-6 Table estimate petrophysical properties for MH-1 | 52 |

LIST OF FIGURE

| FIGURE | PAGE |
|---|------|
| 1.1 Flow chart for log interpretation and formation evaluation | 4 |
| 1.2 Show Wells Location | 7 |
| 1.3 Show Wells Locations Map | 8 |
| 1.4 Show Muglad Rift Basin | 9 |
| 1.5 Show Formation Layers of Muglad rift basin | 10 |
| 3.1 Schematic of down hole measurement environment for several zones (Schlumberger, 1998). | 24 |
| 3.2 Resistivity profile for a transition-style invasion of a hydrocarbon bearing formation (Asquith, G. and Krygowski, D., 2004). | 25 |
| 4.1 showing lithology log and resistivity log | 32 |
| 4.2 Cross-over of thick sand between spectral density and neutron porosity log | 33 |
| 4.1 show relation between Vsh% and IGR | 35 |
| 4.4 show porosity estimation from sonic and Neutron, Density | 36 |
| Appendix-A1 -Lithology and Resistivity logs and saturation layers MH-2 | 53 |
| Appendix-A2 -Lithology and Resistivity logs and Spectral density, Dual spaced neutron MH-2 | 54 |
| Appendix-A 3 -Lithology and Resistivity logs vsh MH-4 | 56 |
| Appendix-A4 -Lithology and Resistivity logs and saturation layers | 57 |
| Appendix-A5 -Lithology and Resistivity logs and Spectral density, Dual spaced neutron MH-1 | 58 |
| Appendix-A6 -Lithology and Resistivity logs and Spectral density, Dual spaced neutron MH-1 | 59 |

| | |
|----------------------------|--|
| a | Tortosity exponent |
| CEC | Cation Exchange Capacity |
| Gg | Geothermal gradient |
| h | Reservoir thickness |
| Ish | Shale Index |
| K | Potassium (percentage) |
| KL | Log derived permeability (mD) |
| m | Cementation exponent |
| mD | mili Darcy |
| N/A | Not Available |
| n | Saturation exponent |
| ppm | Parts per million |
| psi | Pound per square inch |
| ρ_b | Bulk density (g/cc) |
| Rmf | Mud filtrate resistivity (ohm-m) |
| Rt | True resistivity (ohm-m) |
| Rw | Formation water resistivity (ohm-m) |
| Rxo | Flushed zone resistivity (ohm-m) |
| Sw | Water saturation for un-invaded zone (fraction) |
| Swb | Saturation of physically bound water in total Pore Volume, PV (fraction) |
| Sxo | Water saturation for flushed zone (fraction) |
| Swt | Water saturation of the total porosity (fraction) |
| Tcf | Trillion cubic feet |
| Tf | Formation Temperature |
| Th | Thorium (ppm) |
| Ts | Surface Temperature |
| U | Uranium (ppm) |
| Vsh | Shale volume (fraction) |
| Vcl | Clay content (fraction) |
| 2D | Two dimensional |
| OF | Degree Fahrenheit |
| % | Percentage |
| Ω -m | Ohm meter |
| α | Shale effect |
| β | Coefficient |
| ρ_f | Fluid density (g/cc) |
| ρ_{ma} | Matrix density (g/cc) |
| Φ_e | Effective porosity (fraction) |
| ΔT | Sonic travel time (μ s/ft) |
| Elaborations/Abbreviations | |
| API | American Petroleum Institute |
| BGFCL | Bangladesh Gas Fields Company Ltd. |
| BHTV | Borehole Tele-viewer |
| BK | Bakhrabad |
| BVW | Bulk Volume Water (fraction) |
| DD | Driller Depth |
| DELT | Sonic interval transit time (μ s/ft) |
| FMS | Formation Micro-Scanner |
| GIIP | Gas Initially In Place |

| | |
|--------|--|
| GR | Gamma Ray log |
| GRM | Gamma Ray Method for shale volume estimation |
| HCU | Hydrocarbon Unit |
| IKM | Intercomp Management Ltd. |
| KB | Kelly Bushing |
| MHI | Moveable Hydrocarbon Index (fraction) |
| MMSCFD | Million standard cubic feet per day |
| NPHI | Neutron porosity (percentage) |
| NMR | Nuclear Magnetic Resonance Imaging log |
| OBM | Oil Based Mud |
| PHID | Density porosity (fraction) |
| PSOC | Pakistan Shell Oil Company |
| PMRE | Petroleum & Mineral Resources Engineering |
| RDMD | Reservoir and Data Management Division |
| TD | Total Depth |
| TOC | Total Organic Content |
| TVD | True Vertical Depth |
| WBM | Water Based Mud |
| WHP | Well Head Pressure (psi) |

Chapter One:

Introduction

1.1 Introduction

-Formation Evaluation is the practice both the physical and chemical properties of rocks and the fluids they contain. The objectives of Formation evaluation are to evaluate the penetrated or absence of commercial quantities of hydrocarbon in Formation penetrated by the wellbore, to determine the static and dynamic characteristics of productive reservoir, detect small quantities of hydrocarbon which nevertheless may be very significant from an exploration standpoint, and to provide a comparison of an interval in one well to the correlative interval in another well. It can be performed in several stages such as during drilling by mud logging, logging while drilling, during logging (quick look log interpretation) and After logging (detailed log interpretation), by core analysis in the laboratory, etc.

- Wire line logs are one of the many different sources of data used in Formation evaluation. Due to accurate depth determination and near proximity of receiver to Formation wire line logs (both conventional and special logs which include Formation Micro-Scanner (FMS), Borehole Tele-viewer (BHTV), Deep-meter logging, Nuclear Magnetic Resonance (NMR) Imaging logs, etc.).

From log data analysis, estimated petrophysical properties give the significant information about formation, and help to make the decision of whether to set pipe and perforate or consider abandonment still hangs.

- These properties are shale volume, porosity, permeability, formation resistivity and water saturation. Calculated values of water saturation only provide the analysis with information about fluids are present in the formation to interest. In many cases, water saturation is not reflection of relative proportions of fluids that may be produce.

- Therefore, when making the decision to set pipe or abandon, all available information should be taken into account. Water saturation should be the basis for that important decision making process such as irreducible water saturation, bulk volume water and moveable hydrocarbon, etc. the petrophysical properties such as porosity, and sand thickness and hydrocarbon saturation is important for estimating of hydrocarbon reserves, and reservoir performance analysis.

1.2 Objectives of the study:

- The main objective of the present study is formation evaluation of **(Bentiu formation evaluation in hamra oil-field by using Wireline Logs)**

that is to ascertain the followed parts:

- 1- Lithology identification and detection of hydrocarbon bearing zone.
- 2- Estimation of shale volume and reservoir thickness.
- 3 - Assessment of effective porosity.
- 4 - Determination of water saturation.
- 5 - Estimation of log derived permeability.
- 6 - Comparison of petro physical properties of this reservoir with different studies.

1.3 Methodology

- In manual interpretation of the available wire line log data and formation evaluation, some standard rule and practices used in the current study, which mentioned as below.

1.3.1 lithology identification and hydrocarbon bearing zone detection

- Lithology has been identified from spectral and natural gamma ray (GR) log response.
Hydrocarbon bearing zone is detected by resistivity log and porosity comparing GR log response.

1.3.2 Estimation of shale volume and reservoir thickness

- Shale volume (Vsh) has been calculated individually form spectral and Natural Gamma Ray log, and resistivity methods

1.3.3 Assessment of porosity

- Porosity has been calculated from Neutron log, Density log and sonic log individually. Then Neutron-Density combined formula has been applied

with clay corrected (HLS Asia limited, 2008) and the arithmetic average porosity is estimated for further interpretation.

1.3.4 Geothermal gradient and formation temperature

- These have been calculated from Arps formula (HLS Asia Limited, 2008).

1.3.5 Formation water saturation

- Formation water resistivity (R_w) has been calculated from Inverse Archie's method (R_{wa} analysis). Then estimated R_w is corrected for formation depth which is used for estimating water saturation (HLS Asia Limited, 2008; Miah, M.I. and Howlader, M.F., 2012).

1.3.6 Determine of water saturation

- Water saturation has been estimated from Archie's formula (Archie, 1942).

1.3.7 Moveable hydrocarbon index and bulk volume water

- Moveable hydrocarbon index (MHI) is the ratio of SW_u (water saturation of un-invaded zone) and SW_f (water saturation of flushed zone). Hydrocarbon bulk volume water (BVW) has been estimated from Archie's formula, then the sand grain size has been estimated from BVW range (Asquith, G. and Krygowski, D., 2004).

1.2.8 Log derived permeability

It has been calculated using Wyllie & Rose equation (Crain, 1986).

The summarized methodology of formation evaluation has been shown in the flow chart in, Figure 1.1 (Asquith, G. and Krygowski D., 2004; Hamada, 1996).

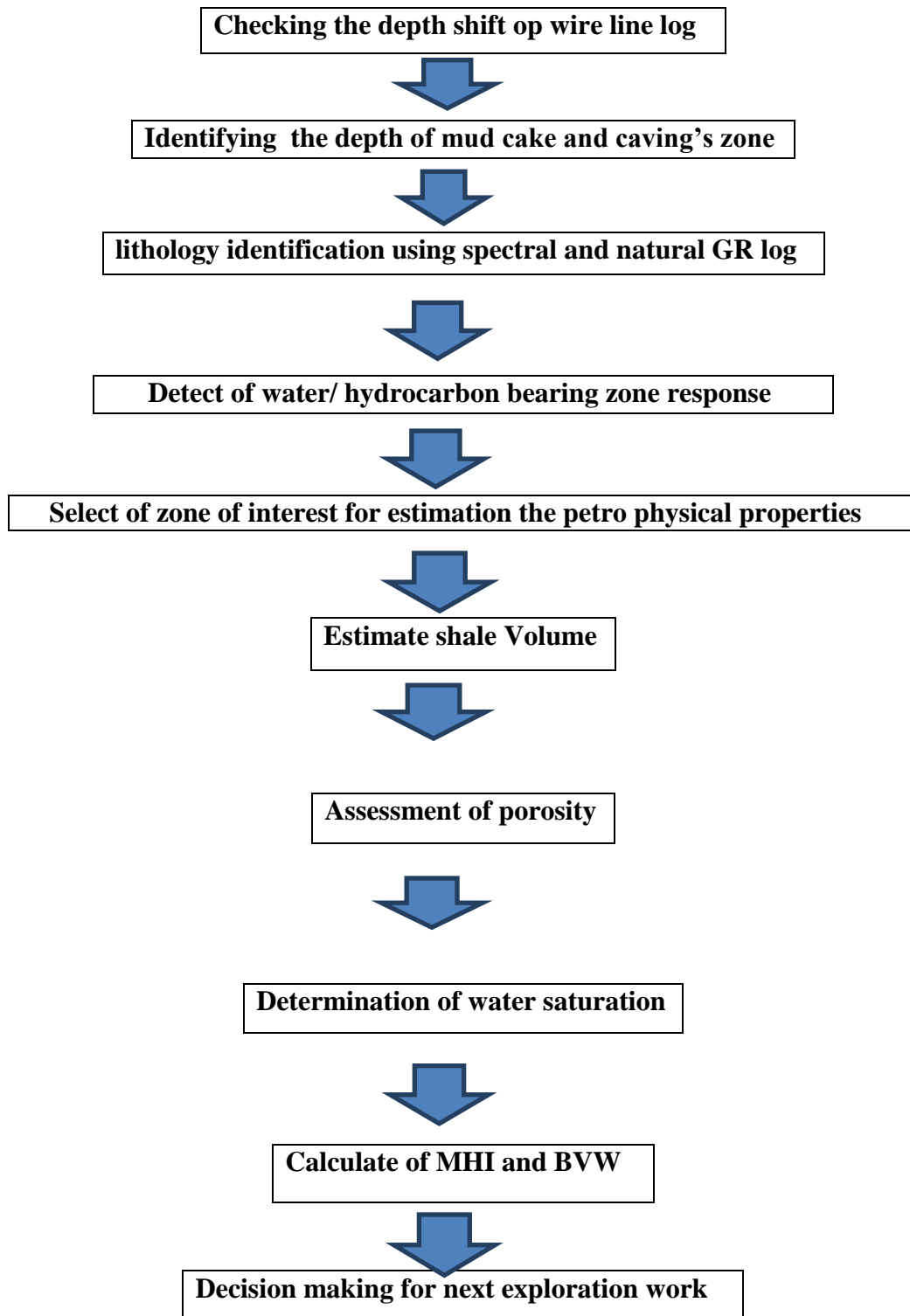


Figure 1.1Flow chart for log interpretation and formation evaluation

OVER VIEW ABOUT MH OIL FIELD

1.4 location of study area:

- The muglad rift basin is the largest of central African rift basins located in southwest

central Sudan. It covers an area about (120,000 km²) and is up to (200 km) wide and over (800

km long). Locally the basin contains up to (13 km) of cretaceous to tertiary sediments. It

extends from western cordovan, to southern Darfur states. In the it contains a number of

hydrocarbons accumulations of various sizes largest of which in the northwest of unite state

south central of muglad rift basin. It is bounded approximately by latitudes (09 degree 17sec N) and longitude (29 degree 5sec) and (29degree 10sec E). Muglad basin is a rift basin

developed in Mesozoic –Cenozoic time and was intended as an extensional basin or graben

(half graben) to the direct south of central Africa shear zone (CASZ). The muglad town it's in

western kordufan state. Muglad town represent the center of the messeria tribe.

-Three wells from the study area(MH#) were selected fault the present study namely:

1.5 Accessibility

- The study area is linked with Khartoum by a railway which passes through sennar, Kosti, ErRahad to Babanusa and then runs southward through the Muglad city to Wau. Also from Babanusa a line runs westward via the NW Muglad Basin up to Nyala. A paved road runs from Khartoum to Kadugli through EL Obeid, but rom EL Obeid many unpaved roads can be followed to different towns and villages in the area. These passageways cross thick forest and mountainous areas and are passable

only during the dry season. Also we could reach it by airplanes which are safest, fastest and more reliable compared to ground roads.

1.6 Topography

-The topography of the study area is characterized by sand dunes which occupy more than 65% of the northern parts of Darfur and about 10 to 15 % of southern Darfur. The region is characterized by gently undulating to nearly level uplands; however, it is interspersed with various hills such as Meidoub and Tagabo. Clay and Gardud soils occupy the western and south western parts and some area in the north.

1.7 Drainage

-The White Nile and its tributaries which are Bahr El Arab, Bhar El Gazal, and Bhar EL Zaraf are the major drainage in the area. The White Nile is flowing across the southern and the eastern parts of the White Nile River is called Bahar El Jabal. The Kordoan and Darfur surface water drainage systems are mostly seasonal streams. Khor Abu Habel and WadiKhdari represent the most significant drainage system in the area. Some of the small spring-fed streams and of the ephemeral wadis and Khors which carry runoff reach the White Nile or its perennial tributaries.

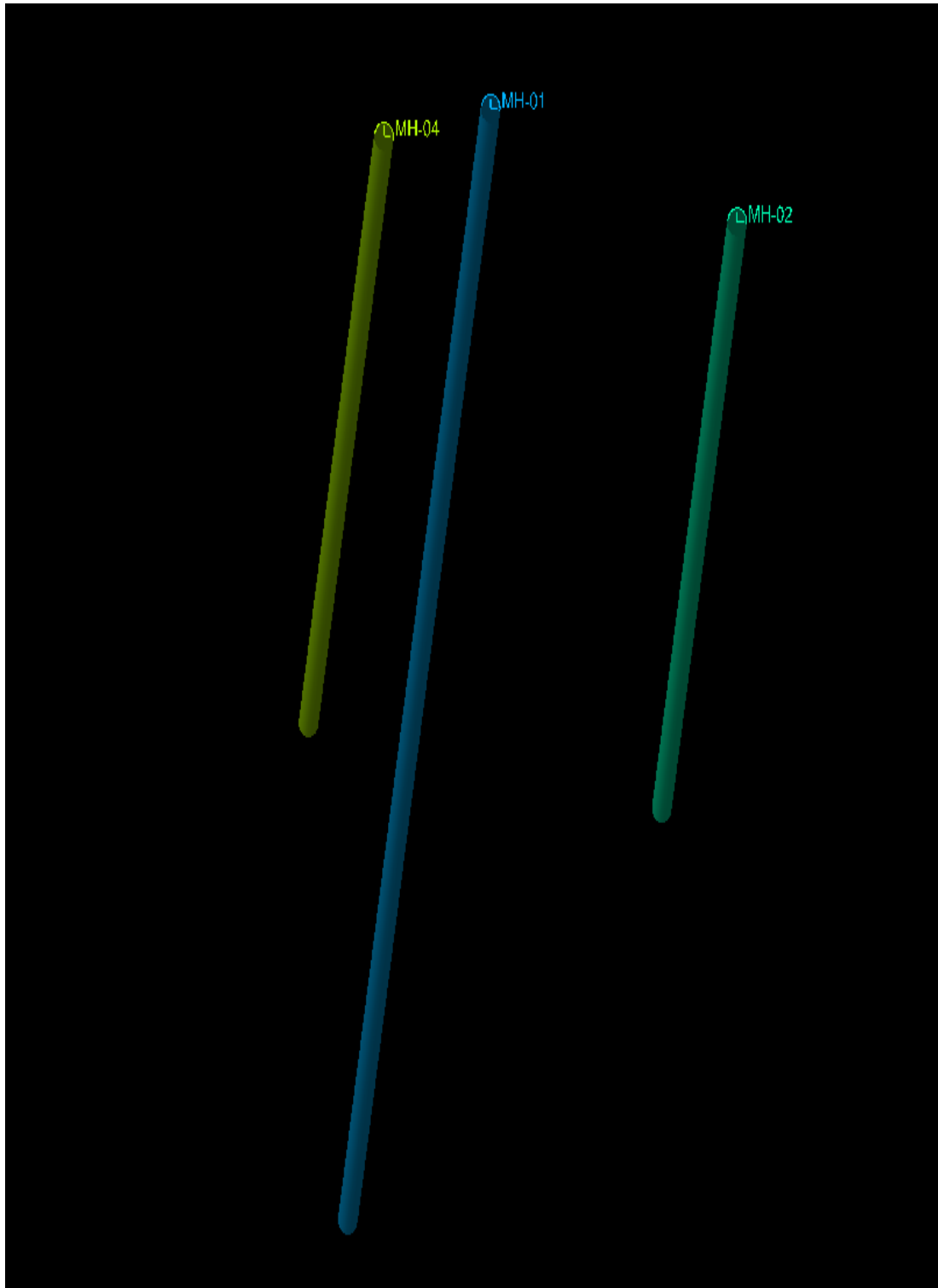
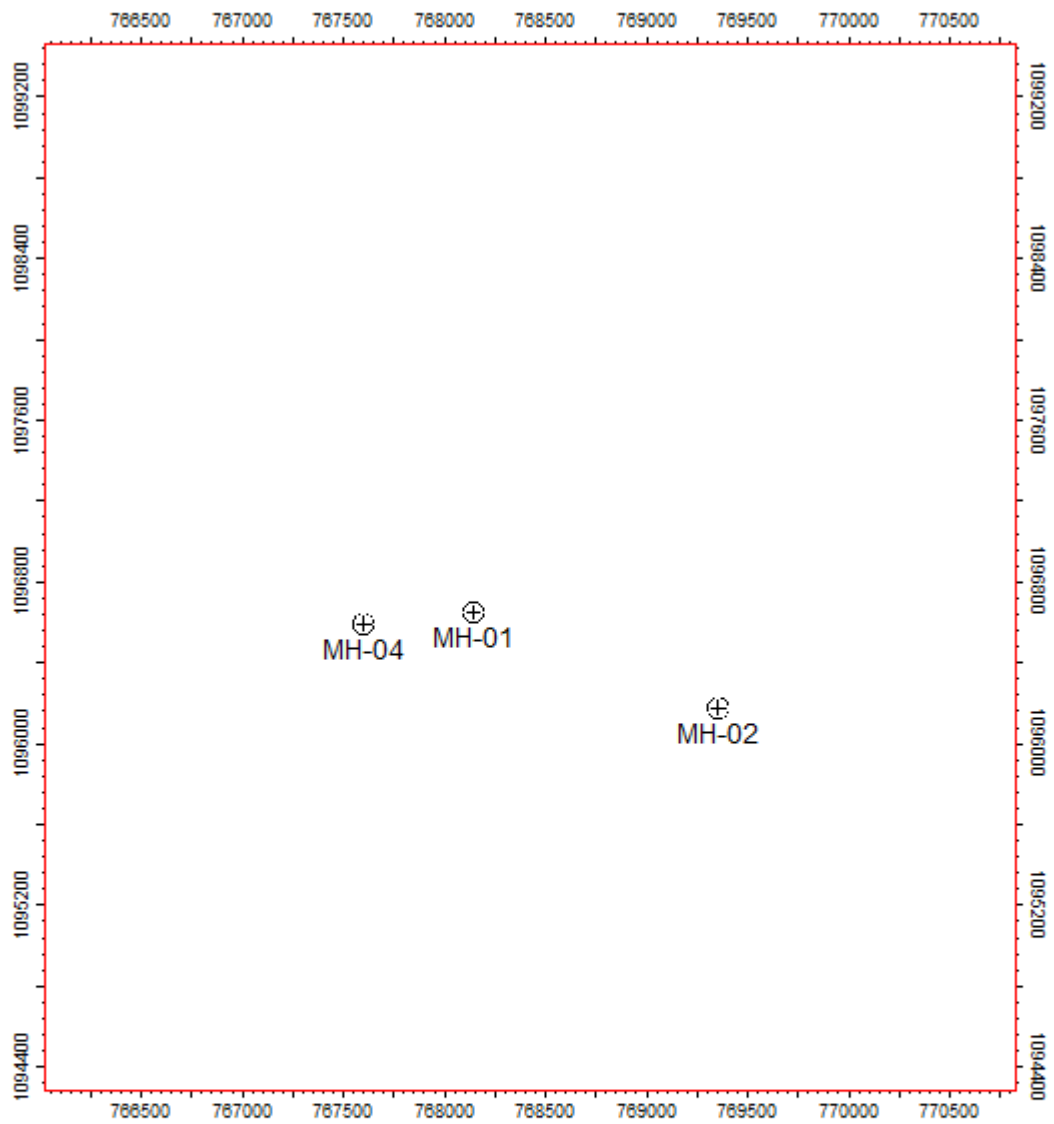


Figure 1.2 Show Wells Location



| Map | |
|--------------|--------------------|
| Country | Scale 1:32000 |
| Block | Contour inc |
| License | User name Admin |
| Model name | Date 05/14/2017 |
| Horizon name | Signature |

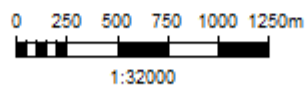


Figure 1.3 Show Wells Locations Map



Figure 1.4 Show Muglad Rift Basin

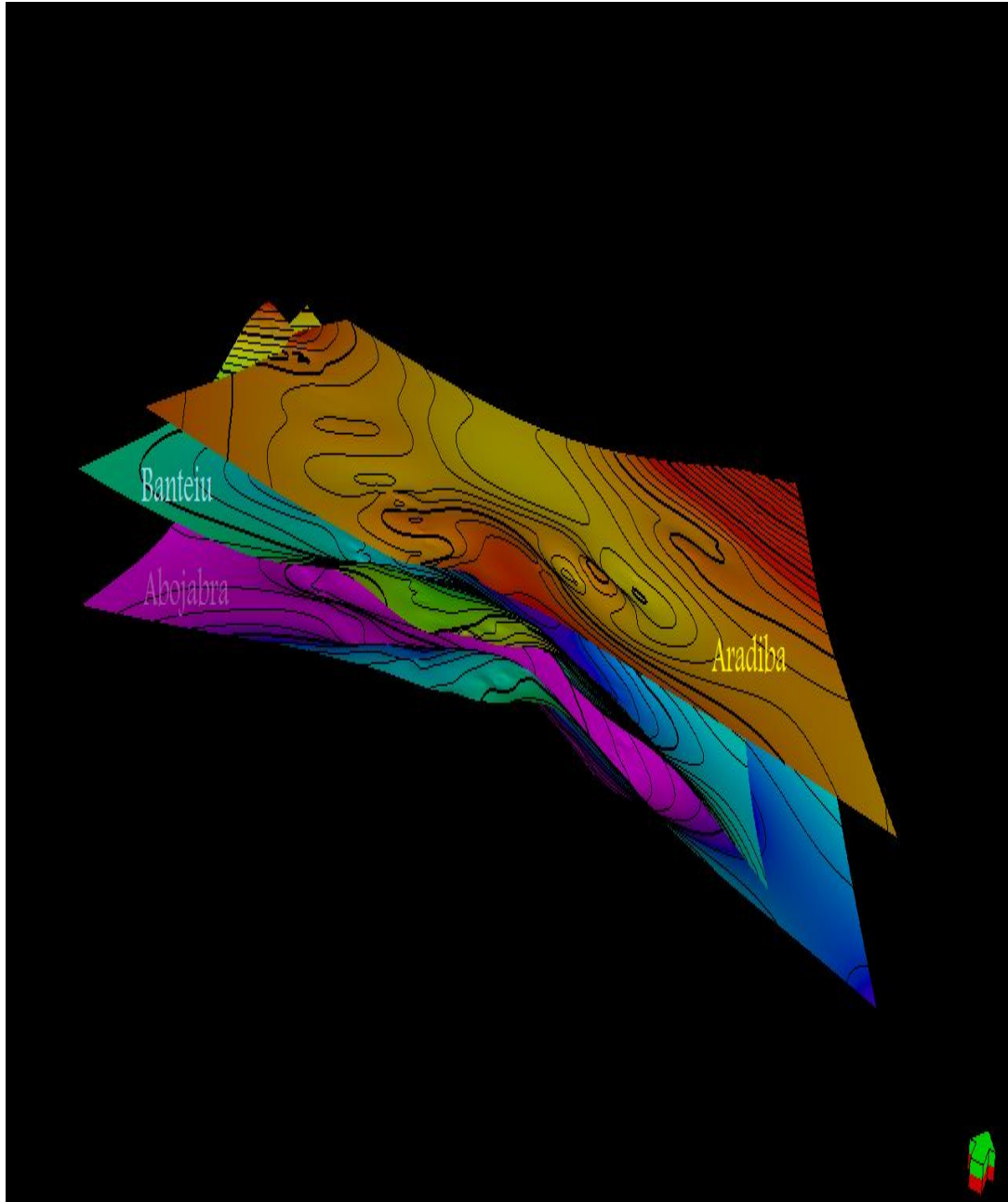


Figure 1.5 Show Formation Layers of Muglad rift basin

Chapter Two:

Literature Review

The literature review and method of investigation

2.1 historical background of oil and gas exploration in Sudan:

- Oil exploration in Sudan started in 1959, when Italy's Agip oil company was granted concession in the red sea area, carrying out seismic survey and drilling six well. Following Agip into the red sea, France's Total, Texas Eastern, union Texas Chevron. All yield nothing for the next fifteen years.

The only successful results were achieved by Chevron in 1974, 120KM southeast of Port Sudan.

Where dry gas and gas condensate were found of Bashir-1 and Suaken-1 well. Chevron estimated possible production of some cubic feet of only gas and one thousand barrels of gas condensate per day.

No oil was found, however and most companies relinquished their concessions in the region. Since 1991 the main holder of the red sea concession has been IPC (International Petroleum Corporation). Nov 1991 part of the Swedish London group.

Exploration for oil in Sudan southwest Sudan began in 1975, when the government of Sudan granted Chevron a concession area of 516,000 KM² in block around Muglad and Melut.

Chevron started geological and geophysical survey in 1976, and drilled its first well in 1977, which dry. In 1979, chevron its first oil discovery in Abu Jabra #1, west of Muglad where on 8 million barrels reserve and 1,000 barrels per day (b/d) production rate estimated.

In 1997 Greater Nile Petroleum Operating Co.td (GNPOC), a consortium composed of China National Petroleum Corporation (CNPC), and PETRONAS, oil and neutral gas corporation (ONGC) and **SUDAPET**

Acquired Block1, 2 and 4 from state oil petroleum and launched an extensive exploration and

development program this led to discovery of 1 billion barrels of additional reserve. Shortly

(GNPOC) initiated numerous field development plans (FDPs), constructed 1610km exported

pipeline, and eventually, export the first Sudanese oil in 1999 the pipeline was built in order to

transport the crude oil from the field to the refinery in Khartoum and then to Bashair in Eastern Sudan.

- Ali Sayed Mohamed Ibrahim (2003)

He investigated the depositional environment, source area and paleogeography of the early Cretaceous (Neocomian .Albian) strata of Sharaf and Abu Gabra formations 1 in the N-W. Muglad rift Basin of interior Sudan. Methods of study included lithofacies analysis, heavy minerals, clay minerals and geochemical analyses. The lithofacies analysis reveals that Sharaf and Abu Gabra formations can be divided into three major units namely fluvial dominated, fluvial lacustrine and lacustrine dominated units. The heavy minerals analysis allowed the subdivision of Sharaf and Abu Gabra Formations into three heavy minerals zones. He suggested that the source rocks of Abu Gabra are mixed igneous and metamorphic rocks of granitic and granodioritic composition whereas, the source rocks of Sharaf Formation are mainly metamorphic of granitic and granodioritic composition.

The clay minerals associations and abundances reveal two distinct zones: upper and lower, which can be correlated laterally across Sharaf and Abu Gabra Formations. The upper zone consists of kaolinite, mixed - layer Smectite/ illite, Smectite, illite and / or chlorite, while the lower zone consists of kaolinite, mixed-layer smectite/ illite, illite and diagenetic processes. Geochemical investigations reveal preferential enrichment and depletion of certain chemical elements in the lacustrine / fluvial environments. The multivariate analysis of the chemical elements of the Sharaf and Abu Gabra Formation, show two clusters; cluster one is dominated by samples from Abu Gabra Formation and cluster two is dominated by Shamf Formation. In spite of their different source rocks, the similarity in the chemical composition shown by source samples in these cluster may be due to similar environmental condition within the lacustrine fluvial system. The heavy minerals, feldspars and clay minerals contents suggest a relationship with facies types and their distribution

- Hanan Abd El Mutaal Hussein (1997)

She investigated in her study Cenomanian-Late Albian continental fluvial Bentiu formation based on data obtained from three exploration wells, in. W Muglad basin. Various methods have been used in the present work including lithofacies, reservoir

quality, heavy mineral and clay mineral analyses. The lithofacies analysis allowed the subdivision of Bentiu Formation into lower, middle and upper parts.

The stratigraphic change of lithological facies and depositional patterns of Bentiu formation reflect mainly both allocyclic and autocyclic controls such as the tectonic activity, climate, drainage system, dispersal pattern and sediment load. Reservoir quality of Bentiu formation is controlled by grain-size and sorting and hence by depositional facies and environments. The facies analysis of Bentiu formation suggests a change in fluvial architecture and sand body geometry, from isolated, vertically stacked, narrow channels, in lower Bentiu formation, to vertically stacked broad channels and sand sheets, in middle and upper Bentiu Formation. It has been found that higher porosity and permeability values are associated with the coarse-grained sandy bedload dominated facies of upper and middle Bentiu Formation. In contrast, relatively lower porosity and permeability values are associated with the high sinuosity, mixed-load meandering stream of lower Bentiu Formation.

The heavy mineral analysis which was carried out on the whole penetration thickness of Abu Sufyan well reveals four distinct zones. The metamorphic rocks are the main contribtional source rock, in addition to the volcanic, plutonic igneous rocks and older sedimentary rocks. The heavy mineral assemblages were affected mainly by tectonism, weathering, transportation, abrasion and intrastratal solution. The clay minerals of Bentiu formation mainly consist of kaolinite, smectite, illite, mixed layer s/i and minor chlorite. The clay mineral assemblages of lower, middle and upper Bentiu Formation show a relationship with lithofacies types and depositional systems.

Abu ObeidaAamirBabiker (2000)

He investigated the facies, depositional environment, source area and paleogeography of the Upper Cretaceous outcropping sediments at the NE margin of the Muglad Rift Basin of the south western Sudan. Methods of investigation included lithofacies analysis, grain size, petrography, heavy minerals and clay minerls analysis. The lithofacies analysis reveals the presence of massive to crudely trough cross-bedded pebble conglomerate facies (Gm, Gt) large and small scale trough cross-bedded sandstone facies (Stl. Sts), planar cross-bedded sandstone facies (Fl/Fm).

These facies belong to four major facies association, namely alluvial fan, major channel/bars, minor channel and overbank/ flood plain facies.

The facies associations show tabular to sheet geometries made of braided channels and bar sequences. The laboratory analysis shows that these sediments are generally poorly sorted, coarse to very coarse grained sandstones. The sandstones are mainly quartz arenites with minor arkosicarenites. These sandstones were cemented by ferruginous and/ or siliceous materials and kaolinitic clays, and all appear to have reduced sandstone porosity significantly. The heavy minerals analysis revealed the dominance of the ultra stable assemblage zircon, tourmaline and rutile over the metastable assemblage staurolite and kyanite. Kaolinite dominated over the other clay minerals smectite, illite and chlorite. The facies, heavy and clay minerals contents of sediments in the study area show similarity to those of the Albian- Cenomanian Bentiu Formation.

- Ayad Mohamed Idriss Abass (2001)

He investigated the penetrated part of Bentiu Formation in order to characterize the facies and depositional environments, to characterize the sandstone composition, diagenetic properties and reservoir quality, and to identify the paleogeographic setting and basin development. The methods followed in this study include subsurface facies analysis based on wireline logs, cuttings and core analyses, and laboratory analyses consisting of heavy mineral analysis, petrographic analysis, clay mineral analysis and scanning electron microscopy (SEM). The lithofacies analysis resulted in dividing the penetrated part of Bentiu formation into three parts: upper, middle and lower according to the difference in the recognized lithofacies. The geometry of these three parts was found to be sheet sandstone bodies. The heavy mineral analysis revealed that kyanite and garnet are the most widely spread heavy minerals in the study area indicating that the source rock are of metamorphic origin.

The petrographic analysis revealed that the sandstones are generally quartzarenite with some subarkoses. They are very fine to very coarse grained, sub-angular to well-rounded and moderately to well sorted. The mean porosity value was found to be 30% and it ranges from 21-35%. Diagenetic features affecting the sandstones are quartz overgrowth, clay infiltration and authigenesis, feldspar alteration and calcite cementation, and dissolution. The clay minerals of the penetrated part of Bentiu Formation consist of kaolinite, smectite, illite, mixed layer S/I and chlorite.

The reservoir quality of Bentiu Formation seems to be controlled by large-scale heterogeneities such as facies architecture, geometry and depositional styles

recognized in lower, middle and upper Bentiu Formation small-scale heterogeneities of influence included sandstone detrital composition, texture, grain size and diagenetic features mentioned earlier.

- Mohamed Abaker Abdalla (2001)

He investigated the facies depositional environment, subsurface facies analysis, source area, petrographical characteristics of reservoir, of Upper Cretaceous (Campanian-Maastrichtian) Ghazal Formation in the Muglad rift basin of interior Sudan. Method of this study included subsurface lithofacies analysis, heavy and clay minerals analysis, petrographical analysis and reservoir evaluation from five wells in Heglig and Unity Field. The lithofacies analysis revealed that Ghazal formation could be divided into three major units, namely fluvial dominated unit, fluvial-lacustrine dominated unit and lacustrine dominated unit. These units are divided into several single-story and multi-story sandstone bodies.

Chapter Three:

Methodology

3.1 Theory of Well Logs and Formation Evaluation

3.1.1 Lithology logs: -

- The first goal of formation evaluation is to attempt to identify the lithology down hole and its depth of occurrence. **The spontaneous potential (SP)** curve and the natural **gamma ray (GR)** logs are recordings of naturally occurring physical phenomena in in-situ rocks. *The SP* curve records the electrical potential (voltage) produced by the interaction of formation connate water, conductive drilling fluid and certain ion-selective rocks (shale). **The GR** log measures the strength of the natural radioactivity present in the formation. Nearly all rocks exhibit some natural radioactivity and the amount depends on the concentration of potassium, thorium, and uranium. Both the SP curve and GR log are generally recorded in left track of the log. They are usually recorded in conjunction with some other log such as the resistivity or porosity log. Indeed, nearly every log now includes a recording of GR log.

The Spectral **Gamma Ray** tool works on the same principal as the gamma ray, although it separates the gamma ray counts into three energy windows to determine the relative contributions arising from Potassium (K), Uranium (U) and Thorium (Th) in the formation. The presence of clay minerals or shale (Table 3.1) in a reservoir may either be good or bad in terms of reservoir quality.

Small amounts of clay minerals (high action exchange capacity, CEC result in higher conductivity and lower resistivity) within the pore space of a reservoir may, because of the increased surface adhesion and capillary pressures associated with such small particle sizes, trap interstitial water. The result can be virtually water-free hydrocarbon production from reservoirs of relatively high calculated water saturation. On the other hand, the presence of a large amount of clay may result in the porosity (PHI) and permeability of the reservoir being reduced to the point where the reservoir becomes non-productive.

All lithology is including limestone and dolomite which may potentially contain some amount of clay minerals. More commonly, however, clay minerals are found associated with sandstone reservoirs. Because of this, log analysts typically make reference to the “shaly sand problem” (HLS Asia Ltd., 2008).

Shale can be classified as the following three types: -

| Clay type | CEC | Bulk density, g/cc | PHI | Minor Constituents Th (ppm) | Spectral GR components | | |
|--------------------------|-----------|--------------------|------|--------------------------------|------------------------|---------|----------|
| | | | | | K (%) | U (ppm) | Th (ppm) |
| K (%) Montmorillonite | 0.8-1.5 | 2.45 | 0.24 | Ca, Mg, Fe | 0.16 | 2-5 | 14-24 |
| iteIllite | 0.1-0.4 | 2.65 | 0.24 | K, Mg, Fe, Ti | 14-24 | 1.5 | <2 |
| Kaolinite | 0.03-0.06 | 2.65 | 0.36 | | 0.42 | 1.5-3 | 6-19 |

Table 3.1 petro physical properties of common clay minerals

.1- Laminated shale refers to thin layers of clay minerals-from a fraction of an inch to several inches in thickness-that are interbedded with thin intervals of sandstone.

2- Structural clay refers to detrital clay minerals that exist as individual grains, clasts, or particles along with the framework grains of a reservoir. This type of clay typically has little impact upon reservoir quality because it does not restrict or block pore throats.

3- Dispersed clay refers to very fine grained particles that exist within the pore space of a reservoir and actually replace fluid volume.

These types of clays, because of their disseminated fibrous and plate-like morphologies, may be very damaging to reservoir quality. The presence of clay minerals in a reservoir may seriously affect some log responses, particularly resistivity and porosity. The end result is an erroneously high value of water saturation, and in some cases a productive reservoir may appear to be wet. Field engineers and log analysts should be able to recognize the effects of clay minerals and be able to correct for their presence to yield more accurate values of water saturation. This emphasizes the need for “shaly sand analysis”. Shale Index (Ish) is calculated from GR logs as the following equations: Shale Content (Ish) or Shale Volume:

$$YV_{sh} = \frac{(X_{log} - X_{min})}{(X_{max} - X_{min})} \quad (3.1)$$

Where: -

Y= GR/K/Th.

Xlog= (GR/K/Th) response in the formation of zone interest.

Xmin= (GR/K/Th) response in clean shale free formation.

Xmax= (GR/K/Th) response in clean shale zone over the entire log.

Using Gamma Ray Method (GRM), Ish as a linear expression of Shale volume, Vsh is most suitable for laminated shales. In this case, the resulting ratio reflects the percentage of clay minerals contained in the reservoir. Again, when this ratio exceeds 15%, then it should be assumed that the formation is indeed shaly sand and that the Archie equation should be abandoned for a technique that will yield better results of water saturation (Sw) in the presence of clay minerals. Some analysts prefer to use Gamma Ray Index, Ish as a shale indicator in all types of shales. However, the relationship between Ish and Shale volume (Vsh) becomes non-linear for both structural clays and dispersed clays. There is a wide variety of non-linear relationships can be found between Ish and Vsh, but none of these is universally accepted (Schlumberger, 1998a).

Shale volume (Vsh) can be calculated from non- linear relationships are listed below (Bassiouni, Z., 1994): For tertiary rocks, the Larionov equation is

$$V_{sh} = 0.083(2^{3.71 * I_{sh}} - 1) \quad (3.2)$$

Shale volume can be calculated from true resistivity method, TRM (Hamada, 1996):

$$V_{sh} = \left[\left[\frac{R_{cl}}{R_t} \right] \times \left[\frac{(R_{tmax} - R_t)}{(R_{tmax} - R_{cl})} \right]^{0.06667} \right] \quad (3.3)$$

Where: -

Rcl = resistivity of clay or shale zone.

Rtmax = the maximum true resistivity over the entire log.

Rt = true resistivity of the zone of interest.

3.1.2 Porosity logs:

Rock porosity can be obtained from the sonic log, the density log, or the neutron log. For all these devices, the tool response is affected by the formation porosity, fluid, and matrix. If the fluid and matrix effects are known or can be determined, the tool response can be related to porosity. Therefore, these devices are often referred to as porosity logs. All three logging techniques respond to the characteristics of the rock immediately adjacent to the borehole. Their depth of investigation is very shallow only a few inches or less and therefore generally within the flushed zone (Schlumberger, 1998a)

may be defined as the measure of void space in the reservoir material which is available for the accumulation and storage of fluids. In general, naturally occurring rocks are permeated with water, oil, gas or combination of these fluids. Absolute or total porosity is defined as the ratio of pore space to the total volume of reservoir rock and is commonly expressed as a percentage.

Two measurements, pore volume and bulk volume are required to obtain the percentage porosity in accordance with the equation. Porosity varies greatly both laterally and vertically within most reservoirs.

- The measurements ordinarily used in reservoir studies is the ratio of the interconnected pore space to the total bulk volume of the rock and is termed effective porosity.

The effective porosity is commonly 5 to 10 percent less than the total porosity. It may also be termed as the available pore space, since oil and gas to be recovered must pass through interconnected voids. Porosity in sandstone varies primarily with grain size distribution and grain shapes, packing arrangement, cementation and clay content. A reservoir having a porosity of less than (5) percent is generally considered noncommercial. A rough field appraisal of porosities is included in below :

| porosity Rang (%) | porosity quality |
|--------------------------|-------------------------|
| 0 - 5 | Negligible |
| 5 - 10 | Poor |
| 10 - 15 | Fair |
| 15 - 20 | Good |
| 20 -25 | Very good |

Table 3.2:Estimate porosity quality

3.1.3 Neutron log:

Neutron logs are porosity logs that measure the hydrogen concentration in a formation. In clean formations (shale free) where porosity is filled with water, oil or gas, the neutron log measures liquid filled porosity (NPHI). Neutrons are created from a chemical source in the neutron logging tool. When these neutrons collide with the nuclei of the formation the neutron loses some of its energy. With enough collisions, the neutron is absorbed by a nucleus and a gamma ray is emitted. Because the hydrogen atom is almost equal in mass to the neutron, maximum energy loss occurs when the neutron collides with a hydrogen atom. Therefore, the energy loss is dominated by the formation's hydrogen concentration. Because hydrogen in a porous formation is concentrated in the fluid-filled pores, energy loss can be related to the formation's porosity. The most commonly used neutron log is the compensated neutron log which has a neutron source and two detectors. The advantages of compensated neutron logs over sidewall neutron logs are that they are less affected by borehole irregularities. When the lithology of a formation is sandstone or dolomite, apparent limestone porosity from compensated neutron log must be corrected to the true porosity using appropriate chart or about 4 porosity unit. Whenever pores are filled with gas rather than oil or water, the reported neutron porosity is less than the actual formation porosity.

This occurs because there is a lower concentration of hydrogen in gas than oil or water. This lower concentration is not accounted for by the processing software of the logging tool, and thus is interpreted as a low porosity. A decrease in neutron porosity by the presence of gas is called gas effect. Also an increase in neutron porosity by the presence of clays is called shale effect (Asquith, G. and Krygowski, D., 2004). Neutron porosity actually increases when clay minerals are added to the reservoir. This result from the fact that clay minerals are hydrated and contain structurally bound hydroxyl ions (OH-) within their crystalline structure. The neutron tool reflects this additional hydrogen as an increase in porosity even though the structurally bound water is not a part of the pore space of the reservoir. It must be remembered that neutron logs sense all of the hydrogen in the formation that includes the hydrogen in the oil, the gas, the water, and the crystalline water. This means it will sense the 48 percent water of crystallinity bound in gypsum crystals and, thus, will calculate out porosity too high. This is also true for other hydrous minerals such as opal, shale or clays in general. Because gas is not very dense, it has a low hydrogen count which yields too low of a porosity. In clay-bearing gas productive zones, the presence of crystalline water causes porosities too high and will mask the presence of the gas (HLS Asia Ltd., 2008). The clay corrected porosity of neutron log can be calculated as the following equation (Asquith, G. and Krygowski, D., 2004).

$$\Phi N, \text{corr} = \Phi N - V_{sh} \times \Phi N, \text{sh} + \text{lithology correction.}$$

Where: -

$\Phi N, \text{sh}$ is the neutron porosity of nearby shale and lithology correction is 0.04 %.

3.1.4 Density log

The density logging tool has a relatively shallow depth of investigation, and as a result, is held against the side of the borehole during logging to maximize its response to the formation. The tool is comprised of a medium-energy gamma ray source (cobalt, cesium 137 and others). Two gamma ray detectors provide some measure of compensation for borehole conditions as like sonic tool. When the gamma rays collide with electrons in the formation, the collisions result in a loss of energy from the gamma ray particle. The scattered gamma rays that return to the detectors in the tool are measured in two energy ranges. The number of returning gamma rays in the higher energy range, affected by Compton scattering, is proportional to the electron density of the formation. Gamma ray interactions in the lower energy range are governed by the photoelectric effect. The response from this energy range is strongly dependent on lithology and only very slightly dependent on porosity. Formation bulk density is a function of the amount of matrix and the amount of fluid in the formation (hydrocarbons, salt or fresh water mud, as well as their respective densities (Beaumont, A. E. et al., 1999; Asquith, G. and Krygowski, D., 2004). It can be expressed as the following equations (Bateman, R. M., 1985; Bassiouni, Z., 1994): Formation bulk density (gram per cubic centimeter).

$$\rho_b = [\Phi \times \rho_f + (1 - \Phi) \rho_{ma}] \quad (3.4)$$

So, density porosity:

$$\Phi_D = (\rho_{ma} - \rho_b) / (\rho_{ma} - \rho_f). \quad (3.5)$$

Shale volume or clay corrected density porosity:

$$\Phi_{D, \text{corr}} = \Phi_D - V_{sh} \times \Phi_{D, \text{sh}}. \quad (3.6)$$

Where: -

$\Phi_{D, \text{sh}}$ is the adjacent clay zone density porosity.

Where:-

$$D, \text{corr} = \left(\frac{\rho_{ma} - \rho_{b, \text{corr}}}{\rho_{ma} - \rho_f \text{ and } \rho_{b, \text{corr}}} \right) = \rho_b + V_{sh}(\rho_{ma} - \rho_{cl}) \quad (3.7)$$

$\Phi_{D, \text{corr}}$ is the clay corrected density porosity.

Effective porosity is that porosity available to free fluids in the reservoir. The values of neutron and density porosity corrected for the presence of clays are then used in the equation below to determine the effective porosity, Φ_e of the formation of interest for gas (Asquith, G. and Krygowski, D., 2004; HLS Asia Ltd., 2008).

$$\Phi_e = \Phi_{N,corr} + \Phi_{D,corr} \quad (3.8)$$

3.1.5 Sonic log

The **sonic log** is a porosity log that measures interval transit time (DELTA T) of a compressional sound wave traveling through the formation along the axis of the borehole. The sonic log device consists of one or more ultrasonic transmitters and two or more receivers. Modern sonic logs are borehole compensated (BHC) devices are designed to greatly reduce the spurious effects of borehole size variations (Kobesh and Blizard, 1959) as well as errors due to tilt of the tool with respect to the borehole axis by averaging signals from different transmitter-receiver combinations over the same length borehole (Asquith, G. and Krygowski, D., 2004). Interval transit time (DELTA T) in microseconds per foot is the reciprocal of the velocity of a compressional sound wave in feet per second. A good correlation often exists between porosity and acoustic interval travel time (ΔT).

According to Wyllie time-average equation (Wyllie et al., 1958).

Total travel time = travel time in liquid fraction + travel time in matrix fraction.

$$\Delta T = \Delta T_f * \Phi + \Delta T_{ma} * (1 - \Phi) \quad (3.9)$$

So, total porosity by sonic log,

$$\Phi_S = \frac{(\Delta T_{ma} - \Delta T_{log})}{(\Delta T_{ma} - \Delta T_f)} \quad (3.10)$$

This equation applicable only for calculation in clean, compacted, and consolidated sandstones. Lack of compaction is usually indicated when the interval transit time of adjacent shales, ΔT_{sh} , exceeds 100 μ sec/ft. The interval transit time of a formation is increased due to the presence of hydrocarbons (i.e. hydrocarbon effect). If the effect of hydrocarbons is not corrected, the sonic derived porosity will be too high. Hilchie (1978) suggests the following empirical corrections for hydrocarbon effect.

$$\Phi = \Phi_S \times 0.7 \text{ for gas.}$$

And

$$\Phi = \Phi_S \times 0.9 \text{ for oil.}$$

3.1.6 Resistivity logs:

The resistivity of a formation is a key parameter in determining hydrocarbon saturation. Electricity can pass through a formation only because of the conductive water it contains. With a few rare exceptions, such as metallic sulfide and graphite, dry rock is a good electrical insulator. Moreover, perfectly dry rocks are very seldom encountered. Therefore, subsurface formations have finite, measurable resistivity's because of the water in their pores or absorbed in their interstitial clay. The resistivity of a formation depends on resistivity of the formation water, amount of water present and pore structure geometry. The units of resistivity are ohm-meters squared per meter (ohm-m). Resistivity tools fall into two main categories such as laterolog and induction type. Laterolog tools use low-frequency currents (hence requiring water-based mud-WBM) to measure the potential caused by a current source over an array of detectors.

Induction-type tools use primary coils to induce eddy currents in the formation and then a secondary array of coils to measure the magnetic fields caused by these currents. Since they operate at high frequencies, they can be used in oil-based mud (OBM) systems. Tools are designed to see a range of depths of investigation into the formation. The shallower readings have a better vertical resolution than the deep readings. Micro-resistivity tools are designed to measure the formation resistivity in the invaded zone close to the borehole wall. They operate using low-frequency current, so are not suitable for OBM. They are used to estimate the invaded-zone saturation and to pick up bedding features too small to be resolved by the deeper reading tools (HLS Asia Ltd., 2008; Darling, T., 2005). Invasion and resistivity profiles are diagrammatic and theoretical, cross sectional views moving away from the borehole and into a formation. They illustrate the horizontal distribution of the invaded and uninvaded zones and their corresponding relative resistivity's. These corresponding resistivity's and down hole measurement, and resistivity profile are illustrated, respectively in Figure 3.1 and 3.2.

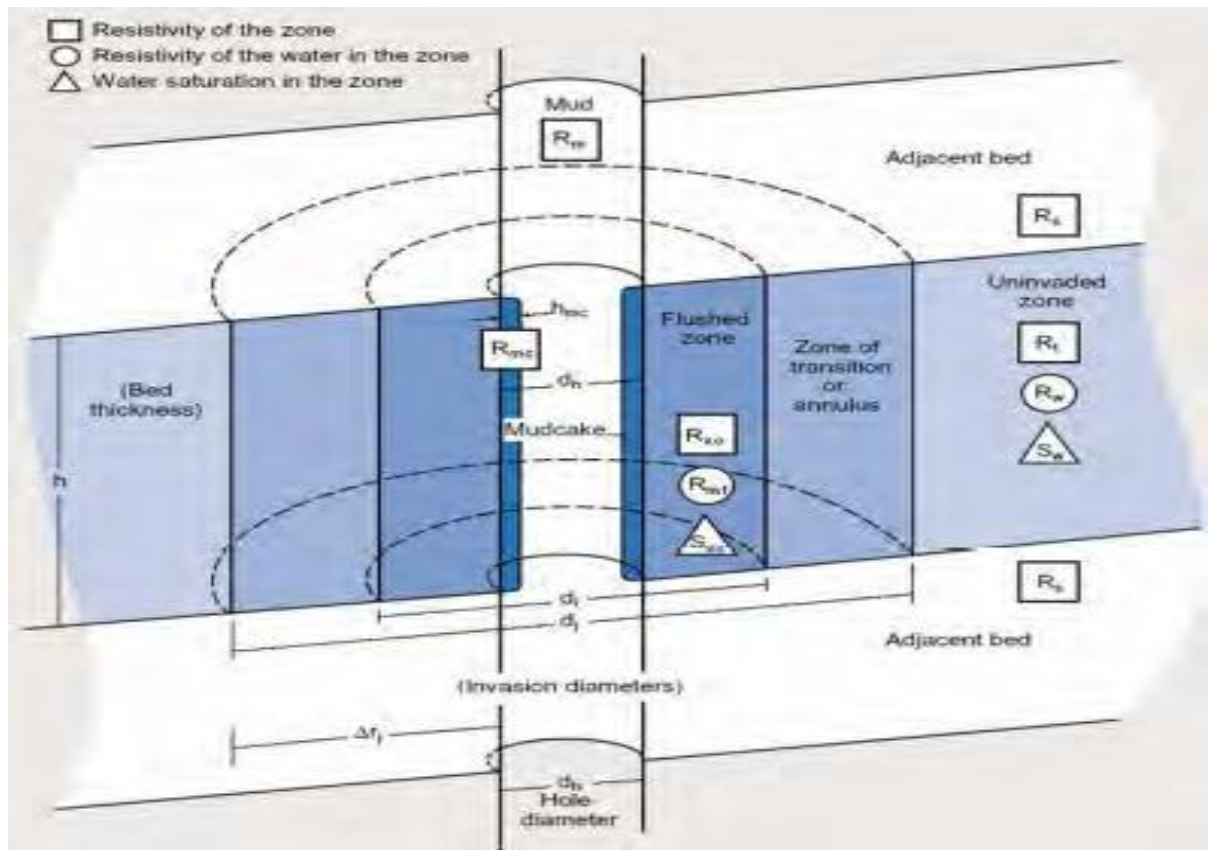


Figure 3.1 Schematic of down hole measurement environment for several zones (Schlumberger, 1998).

Determining water and hydrocarbon saturation is one of the basic objectives of well logging. Hydrocarbon saturation is the fraction (or percentage) of the pore volume of the reservoir rock that is filled with oil or gas. It is generally assumed, unless otherwise known that the pore volume not filled with water is filled with hydrocarbons. Water saturation is defined as the ratio of the volume of water in pore space to the volume of the total pore space (Schlumberger, 1998a).

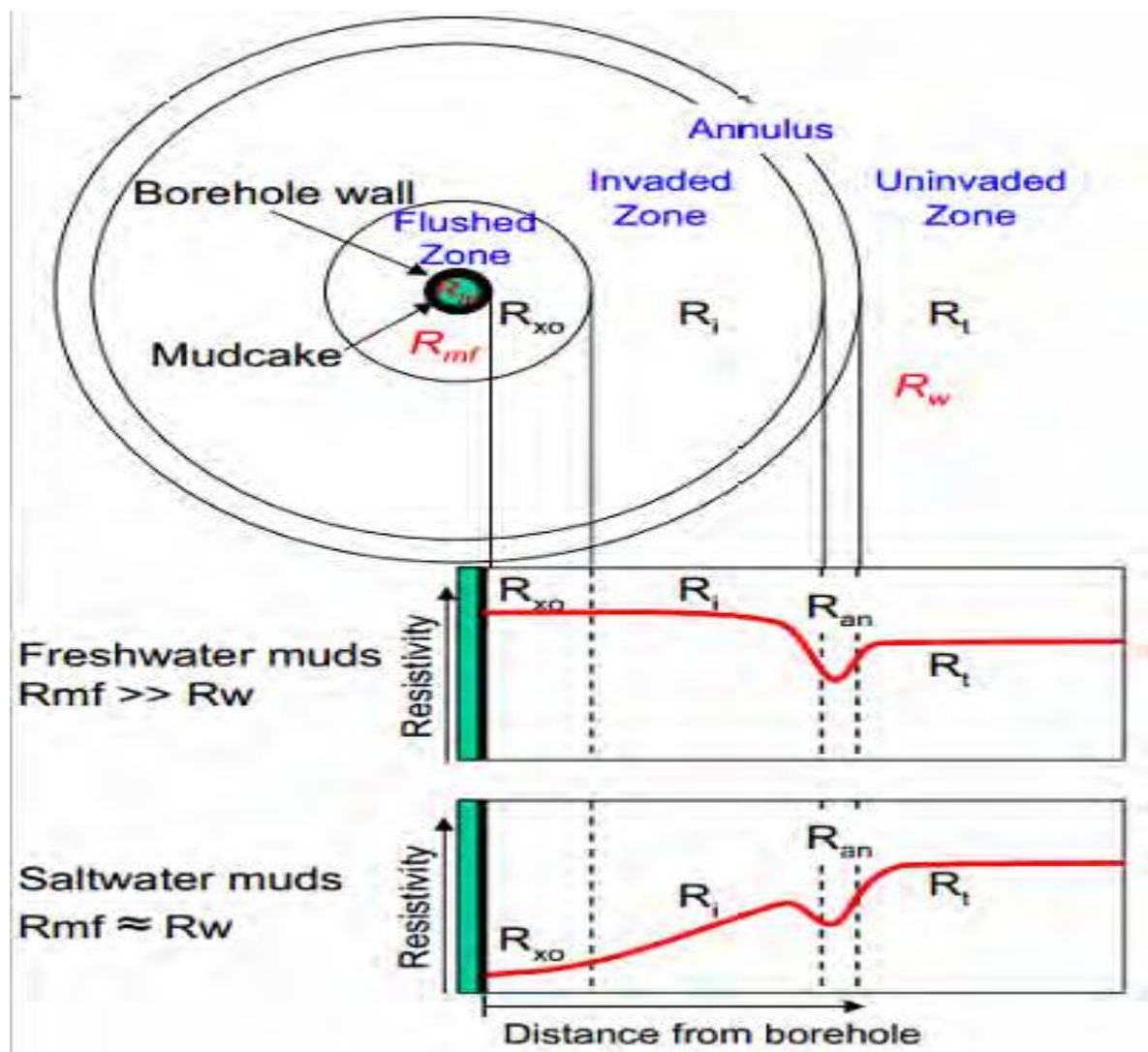


Figure 3.2 Resistivity profile for a transition-style invasion of a hydrocarbon bearing formation (Asquith, G. and Krygowski, D., 2004).

Shaly sand corrections all tend to reduce the water saturation when calculated ignoring the shale effect is ignored in the evaluation processes. Over the years, for shaly sands a large number of models relating fluid saturation to resistivity have been developed according to the geometric form of existing shales (laminated, dispersed and structural). All these models are composed of a shale term and a sand term. All models can be interpreted by clean sand model when the volume of shale is insignificant. For relatively small shale volumes, most shale models might yield quite similar results (Waxman and Smits, 1968; Poupon et al, 1970 and Schlumberger, 1987a). The comparison of the various water saturation equations in shaly sand shows that:

a) the clean sand equation does not compensate for clay conductivity, the water saturation it computes is too high.

b) Indonesia equation (Dresser, 1982) is essentially applicable to laminated clay models, with some adaptation for non-linear behavior of shale electrical properties, Some equations of water saturation estimation are mentioned below:

1) The Archie's water saturation equation for clean sands (Archie, 1942):

$$S_w = \sqrt[n]{\frac{F \cdot R_w}{R_t}} \text{ for un-invaded zone and } S_{xo} = \sqrt[n]{\frac{F \cdot R_{mf}}{R_{xo}}} \text{ for flushed zone}$$

where n is the saturation exponent which is obtained through lithology assumption or data manipulation and core analysis (i.e. for clean, consolidated sands, n=2), R_t is the true formation resistivity for un-invaded zone, R_w is the formation water resistivity and Formation resistivity factor, [F= aΦ^m] where m and n are the tortuosity factor and cementation exponent, respectively (i.e. a=1.0 and m=2.0 for carbonates, (Asquith, G., and Krygowski, D., 2004).

2) The Indonesia model was developed by field observation in Indonesia rather than by laboratory experimental measurement support. It remains useful because it is based on readily available standard log-analysis parameters and gives reasonably reliable results. The formula was empirically modeled with field data in water-bearing shaly sands, but the detailed functionality for hydrocarbon-bearing sands is unsupported, except by common sense and long-standing use. S_w results from the formula are comparatively easy to calculate and, because it is not a quadratic equation, it gives results that are always greater than zero. Several of the other quadratic and iterative-solution models can calculate unreasonable negative S_w results. The Indonesia model (Poupon, and Leveaux, 1971) and other similar models are often used when field-specific SCAL (special core analysis laboratory) rock electrical-properties data are unavailable but are also sometimes used where the SCAL exponents do not measure the full range of shale volumes. Although it was initially modeled on the basis of Indonesian data, the Indonesia model can be applied everywhere. The inputs are the effective porosity (Φ_e), shale volume and resistivity (V_{sh} and R_{sh}), formation water and deep resistivity's (R_w and R_t). The S_w output is usually taken to be the water saturation of the effective porosity, but it has been recently suggested that the output is likely to estimate water saturation of the total porosity, S_{wt} (Woodhouse, and Warner, 2005). Local experience in the Gulf of Suez for Wells 1 and 2 showed that the geometric form of the existing shale is a laminated one. Consequently, the Indonesia equation was used to calculate water saturation in this shaly sand case. Indonesia equation for water saturation estimation (Poupon et al, 1970; Hamada, G. M., 1996) is defined as For un-invaded zones,

$$S_w = (1R_t) [\{V_{cl}(1-0.5V_{cl})R_{cl} * 0.5\} + \{ \Phi e(0.5m)aR_w * 0.5\}] \quad (3.11)$$

and For flushed zone saturation,

$$S_{xo} = (1R_{xo}) [\{V_{cl}(1-0.5V_{cl})R_{cl} * 0.5\} + \{ \Phi e(0.5m)aR_{mf} * 0.5\}]$$

3.1.7 Geothermal gradient and formation temperature

Geothermal gradient (G_g) may also be determined by taking pertinent information from the header and using the following equation (HLS Asia Ltd., 2008):

$$G_g = \left[\frac{BHT - T_s}{TD} \right] \times 100$$

where BHT is the Bottom Hole Temperature in degree Fahrenheit, T_s is the surface (ambient) temperature in degree Fahrenheit and TD is the Total Depth. Once the geothermal gradient (G_g) has been established, it is possible to determine the temperature for a particular depth. This is often referred to as formation temperature (T_f). As with geothermal gradient, T_f may be determined through the use of charts GEN- 2a or GEN-2b (HLS Asia Ltd., 2008). It may also be calculated using the following equation:

$$T_f = [T_s + (G_g \times \text{Formation depth})]$$

3.1.8 Formation water resistivity

Formation water (connate water) is the water, uncontaminated by drilling mud that saturates the porous formation rock. The resistivity of this formation water (R_w) is important interpretation parameters since it is required for the calculation of saturation (water or hydrocarbon) from basic resistivity logs by Inverse Archie's method (Miah and Howlader, 2012; HLS Asia Ltd., 2008) as below equation: .

Formation water resistivity, $R_{wa} = \left[\frac{R_t \cdot \Phi \cdot ND^m}{a} \right]$ for un-invaded zone and Formation mud filtrate resistivity, $R_{mf} = \left[\frac{R_{xo} \cdot \Phi \cdot ND^m}{a} \right]$ for flushed zone. A more straightforward method of correcting resistivity (ohm-m) for temperature is through the use of Arp's equation (Asquith, G. and Krygowski, D., 2004): $R_2 = R_1 \times \left(\frac{T_1 + k}{T_2 + k} \right)$

Where

R_2 = resistivity value corrected for temperature,

R_1 = resistivity value at known reference temperature,

T_1 T_2 = temperature to which resistivity is to be corrected

k = constant value (6.66 for measured temperature in degree Fahrenheit).

3.1.9 Moveable hydrocarbon index

Hydrocarbon movability equation is derived from a comparison of S_w and S_{xo} . The greater the difference between S_w and S_{xo} , the movability is greater (Serra, O., 2007). If the value for S_{xo} is much greater than the value for S_w then hydrocarbons were likely moved during invasion, and the reservoir will produce. An easy way of quantifying this relationship is through the moveable hydrocarbon index, $MHI = \left[\frac{S_w}{S_{xo}} \right]$. Once flushed zone water saturation is calculated, it may be compared with the value for water saturation of the uninvaded zone at the same depth to determine whether or not hydrocarbons were moved from the flushed zone during invasion. If the value for S_{xo} is much greater than the value for S_w , then hydrocarbons were likely moved during invasion, and the reservoir will produce. When MHI is equal to 1.0 or greater, then this is an indication that hydrocarbons were not moved from the flushed zone during invasion of mud filtrate (Asquith, G. and Krygowski, D., 2004; HLS Asia Ltd., 2008).

3.1.10 Bulk volume water

Bulk volume water (BVW) is the product of porosity and water saturation which represents the percentage of rock volume that is water. Water saturation simply represents the fraction of porosity in a reservoir that is occupied by water. In some instances, it may be beneficial to know the fraction of rock volume that is occupied by water. Bulk volume water has several important applications. Within a particular reservoir, BVW may be calculated at several depths. Where values for BVW remain constant or very close to constant throughout a reservoir, this may be taken as an indication that the reservoir is at or near irreducible water saturation (S_{wirr}). Irreducible water saturation is the value of water saturation at which all water within the reservoir is either adsorbed onto grain surfaces or bound within the pore network by capillary pressure. If a reservoir is at irreducible water saturation, then the water present within that formation will be immovable and production will theoretically be water free hydrocarbons. Reservoirs that exhibit variation in values for BVW are typically not at irreducible water saturation and, therefore, at least some water production can be expected. S_{wirr} is related to the grain size of a reservoir. As grain size decreases, the diameters of pore throats within the reservoir will decrease, resulting in higher capillary pressures. This condition implies a reservoir in which a substantial amount of water may be trapped and unable to move. Therefore, when a reservoir is determined to be at irreducible water saturation, values for BVW may be used to estimate the average grain size of that reservoir, (Table 3.3). Realizing the potential for error, this approximation may also be used in reservoirs that are not at irreducible water saturation. The presence of clay minerals in a reservoir also has an impact on values of irreducible water saturation and bulk volume water. As the volume of clay minerals in a reservoir increases, both S_{wirr} and BVW will increase because of the inclination of clay to trap interstitial formation water. If a reservoir is deemed to be at S_{wirr} , then a log derived estimate of permeability can be made. Constant to near-constant values of bulk volume water within a reservoir indicate that reservoir is at (or at least near) irreducible water saturation (HLS Asia Ltd., 2008).

Chapter Four:

Results

RESULTS & DESCUSSION

MH well -2 has been selected for the current research purpose where available log data is listed in Table (4.1). The quality of all log data is good. In the studied well, no depth shift has been found in the logs. No environmental corrections are applied to the aforementioned logs. The potassium (percentage), thorium and uranium (ppm) have been taken from spectral gamma ray log. The Gamma Ray API value is taken from natural Gamma Ray log.

| Log type | Log Name |
|--------------------------|---|
| Borehole measurement log | Caliper log with Bit size |
| Lithology logs | Spectral and Natural Gamma Ray log Self-Potential (SP) log |
| Porosity logs | Spectral density, Dual spaced Neutron, and Sonic Log |
| Resistivity logs | Array compensated true resistivity (Shallow and Deep Resistivity logs) |

Table 4.1 Available log data of MH-2

4.1 Lithology and Hydrocarbon Bearing Zones:

Logging parameters have been taken from log header of the studied well that is shown in Table 4.2. Log reading on each available log curve has been taken with respect to depth and then analyzed. The true resistivity of virgin zone is higher than the shallow zone's resistivity in the sand zone in Figure 4.1. The caliper curve shows mud-cake in the sand zone. This mud-cake indicates that the sand zone is porous and permeable.

Cross over is showing between Neutron and density logs through the hydrocarbon (Gas & Oil) bearing sand zone in Figure (4.2).

There is hydrocarbon (oil) bearing sand zone found from 1531.8m to 1546 m (True Vertical Depth-TVD) based on GR log, resistivity log and porosity log.

:

| Mud Parameters | Value |
|--------------------------------|--|
| Location (m) | LATI 9 45` 27.17` N- LONG 29 27` 22.72`E |
| Drillers depth (TVD) | 1905.8m |
| Logger depth (TVD) | 1901.95m |
| Logged Interval (Top & Bottom) | 1531.8 to 1546 m |
| Casing-Diller | 950,50000 |
| Kelly Bushing Elevation (m) | 7.5 m |
| Bit Size (Inch) | 9.87 (Inch) (F13.4) |
| Type of Fluid | KCL Silicate mud |
| Density & PH | 11.0000 |
| RmandRmf(Ω -m) | 0.0628@145.8F,0.04712Ω-m |
| BHT & Depth | 161.6F |

Table 4.2 Logging parameters of MH-2

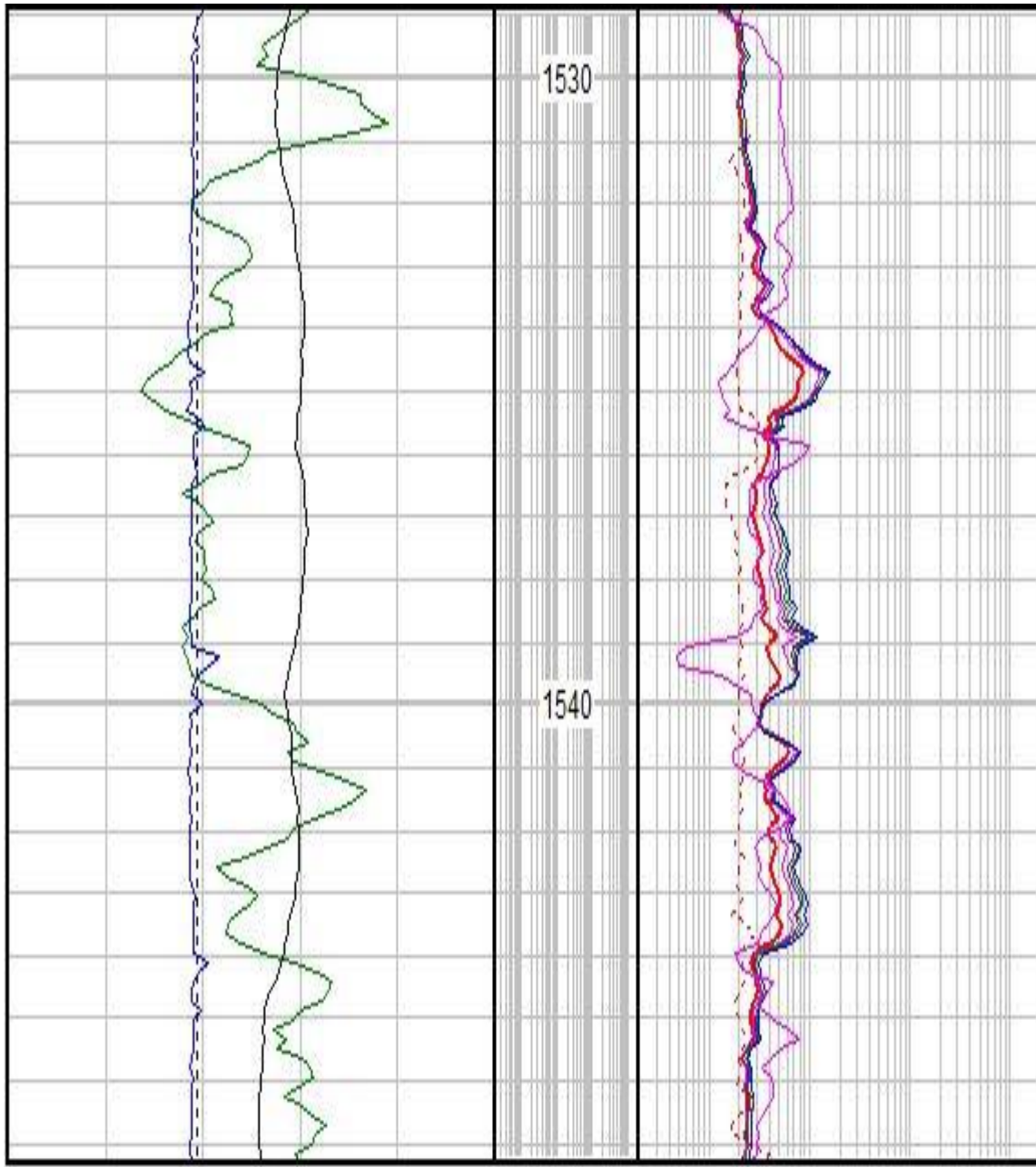


Figure 4.1 showing lithology log and resistivity log .

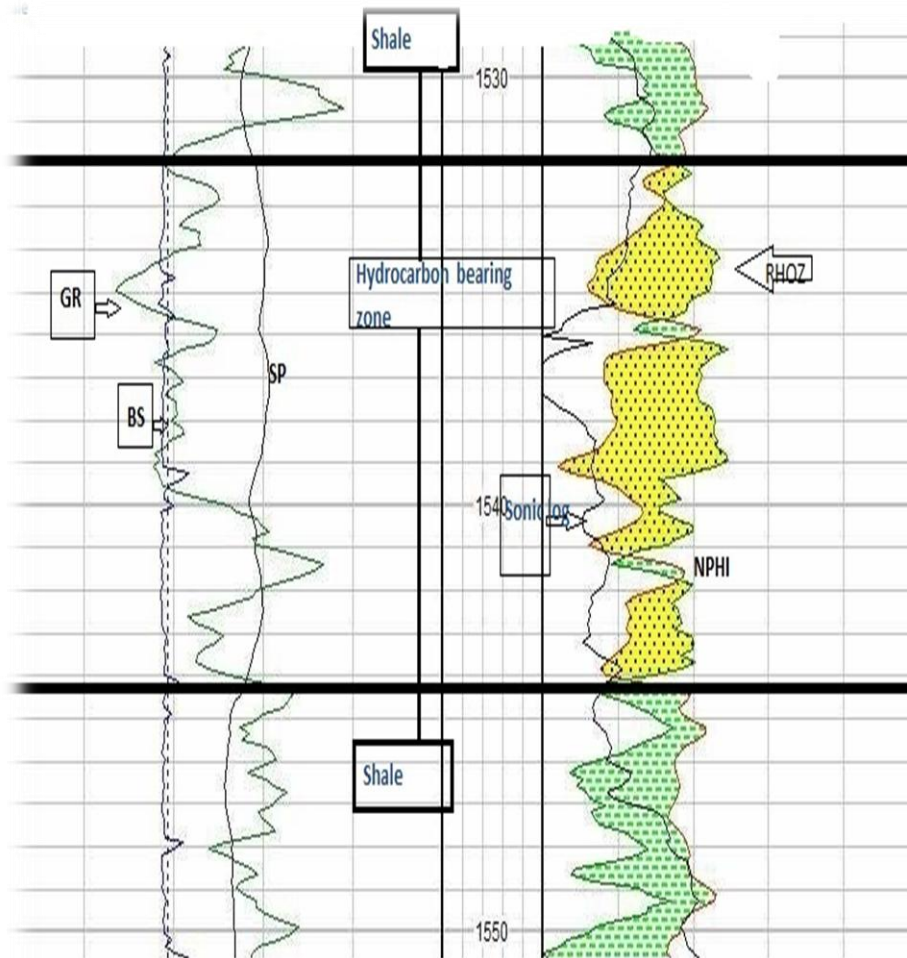


Figure 4.2 Cross-over of thick sand between spectral density and neutron porosity log

The raw data of different well logs of hydrocarbon bearing zone of **MH-2** is shown in Appendix-A1 through A5. The radioactive properties, formation resistivity with bulk density and neutron porosity of sand zone are shown in Table 4.3 for **MH-2**. The true formation resistivity (R_t) and flushed zone resistivity, R_{xo} (ohm-m) have been taken from deep and shallow resistivity logs of this well. The bulk density (RHO_b), photoelectric absorption cross section (Pe) and neutron porosity ($NPHI$) are taken from litho-density and neutron porosity logs, respectively. According to log data analysis of drilled well, the lithology is mainly sand and shale where sand is the dominant fraction. The average bulk density of hydrocarbon the bearing sand are found from the litho-density log as **2.1-2.326gm/cc**. Total thickness of hydrocarbon bearing sand reservoir is **14.2m** which is located at the depth of 1531.8m to 1546m. The depth of hydrocarbon bearing zone are located in Benitu formation mugla Basin.

4.2 Estimation of Shale Volume and Reservoir Thickness:

The true resistivity (R_t) from resistivity log $2.03\Omega m$ (average) of hydrocarbon bearing zone. The ranges of minimum and maximum value of shale index (GR-Ish) and shale volume of hydrocarbon bearing sand is found about 3% to 71% average 26.8% (Tertiary) rocks, respectively.

This value has been used for further estimation of porosity and water saturation. The summarized results are shown in the value of natural gamma ray as GRmin and GRmax are 48 and 102 API at 1535 and 1541 meter, respectively. Table 4.3 and graphically Figure (4.1).

| NO | GRlog | IGR | Vsh % | Depth |
|----|-------|------|-------|--------|
| 1 | 60 | 0.28 | 9 | 1531.8 |
| 2 | 49 | 0.11 | 3 | 1535.3 |
| 3 | 59 | 0.28 | 9 | 1538 |
| 4 | 162 | 0.88 | 71 | 1541 |
| 5 | 89 | 0.70 | 42 | 1546 |

Table 4.3 Estimated shale volume using spectral, natural GR

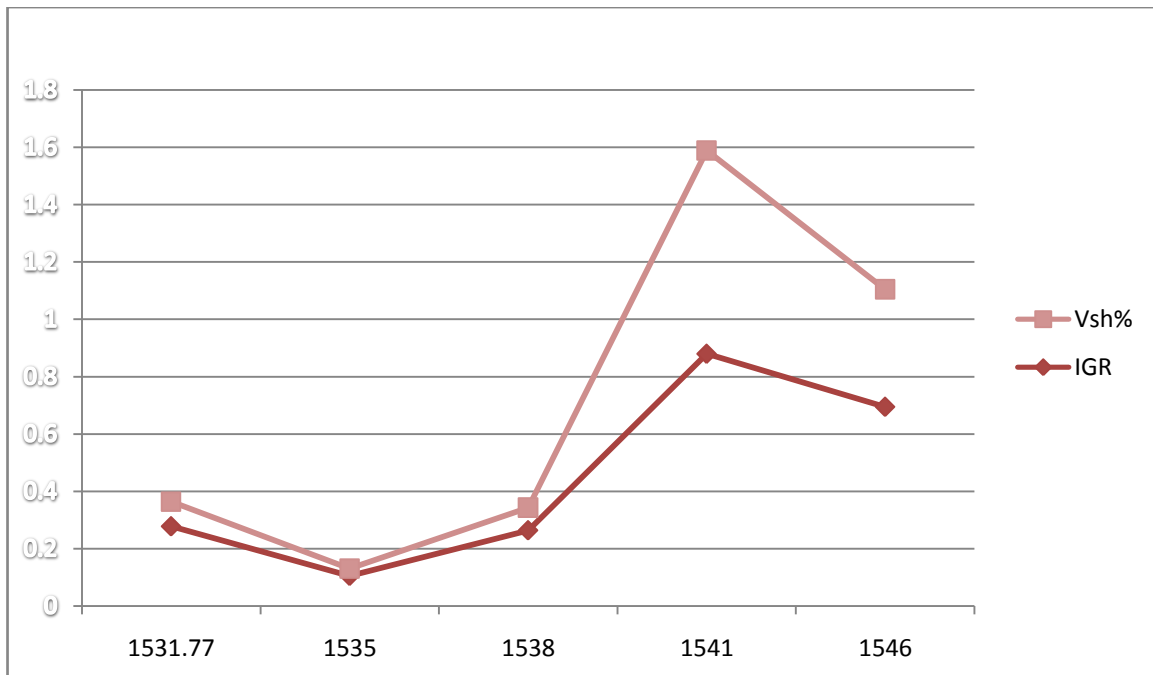


Figure 4.3 show relation between Vsh% and IGR

The aforementioned result shows that the shale volume changed causes for changing the radioactive minerals (Thorium Uranium and Potassium concentration) within formation (Total GR value) with respect to depth. From GR method, estimated arithmetic average shale volume of thick sand is found about 26.8 percent. The gross thickness of thick sand is 14.2m (1531.8m-1546m) where net thickness is 14m. The Net to Gross ratio has been estimated to be 0.716 based on spectral and natural GR log.

4.3 Assessment of Porosity:

Porosity has been estimated from single log methods as well as from Neutron-Density combination formula. In this method, individual porosity from Neutron, Density and Sonic logs have been calculated and compared with each other. In order to interpret and analyse the log data, matrix travel time (ΔT_{ma}) of 55.5 μ s/ft and matrix density (ρ_{ma}) of 2.65gm/cc (Schlumberger, 1998a) has been used for porosity assessment in sandstone reservoir. The fluid density (ρ_f) of 1.0 gm/cc and fluid travel time (ΔT_f) of 189 μ sec/ft (Schlumberger, 1998a) has been used for porosity estimation. The summarized results of porosity are shown in Table 4.4 and graphically represented in Figure 4.2. table 4.3 Estimated porosity from Neutron, Density

| NO | GR | Vsh % | Φ_N | Φ_N correct | ρ_p | Φ Density | Depth |
|----|-----|-------|----------|------------------|----------|----------------|---------|
| 1 | 60 | 9 | 26.89 | 18.79 | 2.326 | 20 | 1531.77 |
| 2 | 48 | 3 | 20.64 | 32.9 | 2.1 | 33 | 1535 |
| 3 | 59 | 9 | 11.59 | 29.09 | 2.147 | 30 | 1538 |
| 4 | 102 | 71 | 28.102 | 21.2 | 2.114 | 32 | 1541 |
| 5 | 89 | 42 | 29.13 | 13.93 | 2.315 | 20 | 1546 |

Table 4.4 Estimated porosity from Neutron, Density

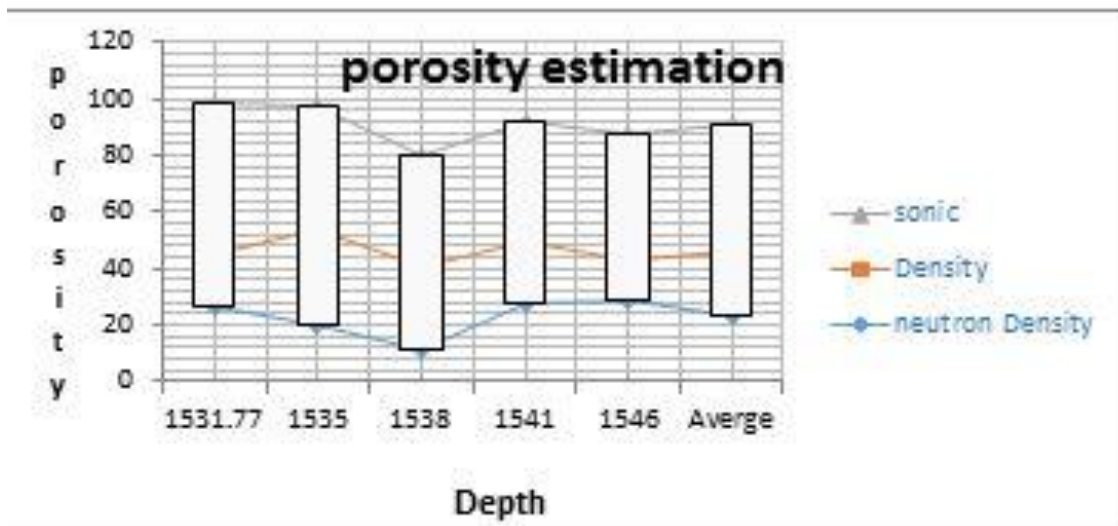


Figure 4.4 show porosity estimation from sonic and Neutron, Density

| NO | Δt_m Log | Δt_{ma} | Δt_{mf} | Φ_e | Φ_e correct |
|----|------------------|-----------------|-----------------|----------|------------------|
| 1 | 110 | 189 | 55.5 | 0.59 | 0.532 |
| 2 | 123 | 189 | 55.5 | 0.49 | 0.441 |
| 3 | 130 | 189 | 55.5 | 0.44 | 0.396 |
| 4 | 124 | 189 | 55.5 | 0.48 | 0.432 |
| 5 | 122 | 189 | 55.5 | 0.5 | 0.45 |

Table 4.5 Estimated porosity from sonic log

The sonic log generally gives higher porosity because of oil and gas effects. The total porosity from sonic log is 50% but corrected sonic porosity for oil effect is 44.9% by Hilchie formula in thick sand reservoir. Among oil sand the combination formula gives average neutron and density porosity ranges are 13.9-29.09% and 20-30% respectively, this porosity quality is good for this oil pool.

4.4 Geothermal Gradient and Formation Temperature:

The determined geothermal gradient and formation temperature of the studied well is shown in Appendix-E1. From the log data analysis, it is found that the geothermal gradient is (0.01) 0F per 100 meter of **MH-2** with average formation temperature of thick sand depth interval of 145.76 to 161.60F. From the analysis, it is found that this (1531.8-1546mTVD) **well shows lower geothermal gradient**, the geothermal gradient and formation temperature are varied with respect to depth of the formation.

4.5 Formation Water Resistivity:

As stated earlier that formation water resistivity (R_w) has been calculated from Inverse Archie's method (R_{wa} analysis) where tortousity factor (a) of 1.00 and cementation exponent (m) of 2.25 has been used. The data has been taken from water bearing sand of the well for R_{wa} analysis. The minimum value of R_w is **0.10** and mud-filtrate resistivity (R_{mf}) is **0.151** ohm-m has been found in interval from 1531.8 to 1546 meter (TVD). Finally considering this interval, R_w and R_{mf} have been calculated for hydrocarbon bearing sand and then corrected for formation temperature with respect to depth. The average formation water resistivity has been found as (**0.042**) ohm-m by R_{wa} analysis.

| Thickness(meter) | Archie's formula (average, %) | | Indonesia model (average, %) | |
|-------------------|-------------------------------|----------------|------------------------------|--|
| | R _{wa} | R _w | R _{mf} | R _w |
| 14.2m | <u>0.023</u> | <u>0.04</u> | 0.151 | Take minimum value of R _w 0.10 |

Table 4.6 Estimated Resistivity water saturation from different models

4.6 Determination of Water Saturation:

Tortuosity (a), saturation (n) and cementation exponent (m) value of 1.00, 2.00 and 2.00 has been used for water saturation estimation for hydrocarbon bearing sand of this well, (Schlumberger, 1998a).

| Thickness (meter) | Archie's formula (average, %) S _w % | Indonesia model (average, %) S _w % |
|-------------------|---|--|
| 14.2m | <u>0.41</u> | 0.608 |

4.7 Estimated water saturation from different models

From the Archie's equation, it is found that average water saturation is about **41%** at a depth (1531.8m-1546m). This value of water saturation are also confirmed by Indonesia modal.

The amount of hydrocarbon (Oil) saturation value from Archie's formula and Indonesia model are **(0.41)** and **(0.608)** percent respectively.

Indonesia equation model give more reliable saturation value than Archie's formula because this reservoir is almost shaly sand reservoir, On the other hand, Archie's formula gives better estimation of water saturation for clean sand reservoirs of any formation. This fluid saturation is most important for reserve estimation and reservoir data analysis of this well.

4.7 Moveable Hydrocarbon Index and Bulk Volume Water:

The average moveable hydrocarbon index (MHI) of reservoir sand is **0.59** by Archie's formula and (0.392%) from Indonesia equation which is an indication that hydrocarbons were moved from the flushed zone during invasion of mud filtrate. So, hydrocarbon is moveable within sand reservoir of this formation.

The BVW (Product of porosity and water saturation) has been estimated from Archie's formula, and Indonesia model water saturation of oil sand which **0.16%**-**0.191%** respectively.

4.8 Log Derived Permeability:

The permeability of the reservoir sand has been calculated using Wyllie & Rose equation assuming irreducible water saturation, Swirrof 1%, permeability constant (CPERM) of 8581 (RPS Energy, 2010), irreducible saturation exponent (EPERM) of 2.00, and porosity constant (DPERM) of 4.40, respectively. Using the above parameters to estimate **Permeability** rock 27.01mD .

4.9 Comparison of Petrophysical Properties with Different Studies:

| parameter/properties | current study | | |
|-------------------------------|---------------|--------|-------|
| | MH-1 | MH-4 | MH-2 |
| Oil or Thick sand interval, m | 30.3 | 7.8 | 14.2 |
| Net Pay, ft. | 30 | 7.2 | 14 |
| Vsh (%) average | 37.08 | 12.85 | 26.8 |
| Φ_n (%) | 22 | 42.8 | 23.27 |
| Sw (%) | 0.29 | 0.16 | 0.41 |
| Rw (Ω -m) | 0.025 | 0.032 | 0.04 |
| Rt (Ω -m) | 23.6 | 4.646 | 2.03 |
| KL (mD) | 27.5 | 265 | 27 |
| MHI | 0.372 | 0.231 | 0.488 |
| BVW | 0.0638 | 0.0685 | 0.09 |

4.8 Comparison of Petrophysical Properties with Different Studies

4.10 Justification and Uncertainty of the Results:

The available logs are interpreted and analyzed using different methods and different approaches. Each method has some limitations in their applicability. Some uncertainties are also there in assumption and application for formation evaluation of this well. Some error may also be there in picking the correct log values. However, uncertainty on logs as well as on the analytical procedure has been described under the following headings:

- Shale volume: This may be changed due to heterogeneity of radioactive minerals within the formation.
- Porosity assessment: Single log porosity method and Neutron-Density combination formula have been used for porosity estimation. Individual porosity logs give big differences of porosity values. Cross-Plot method (gives best result other than core) could not be followed as pure water bearing zones are uncommon in the studied well. The assumed values of both fluid and matrix density, and travel time may be changed due to inhomogeneity of the lithology. Porosity from core analysis is more reliable than the aforementioned methods.

Formation water resistivity and selection of exponents: The water bearing clean sands are uncommon in the studied well. As a result, the estimation of corrected R_w may be wrong due to changing of cementation exponent (m) and actual sub-surface formation temperature. This is an important parameter for estimation of formation water saturation. These exponents ($a=1$, $m=2$ and $n=2$) are critical in calculating porosity, formation water resistivity and water saturation of flushed zones as well as un-invaded zones.

The estimated log derived average permeability from Wylie-Rose method has been estimated as 27.06 mD which is a good permeability for sand reservoirs.

So the oil pool of this formation is potential for production oil

Chapter Five:

Conclusion & Recommendations

5.1 Conclusions

Based on the log interpretation and formation evaluation using available wireline log data for **MH-2** well, the conclusions are as follows:

- Thick Oil bearing sand (Oil sand) is the main reservoir of this well where lithology is mainly medium to coarse grained sand with shale of laminar type and silt. The average Gamma Ray and resistivity ranges are 49-102 API and 2.03 ohm-m (average) of reservoir sand where shale content is about 3% and 71 % from Natural Gamma Ray.
- Neutron-Density combination formula gives better effective porosity value of shaly sand reservoirs which is about 11.5-29.13% as compared to the single log method. This is good quality porosity of this formation.
- Log analysis shows that the average formation water resistivity (R_w) of thick Oil bearing sand is 0.03 ohm-m from R_{we} analysis and formation salinity is about 55000.00000 ppm with R_w of 0.042ohm-m.
- Indonesian model give a pessimistic value of water saturation of virgin zone in thick sand as 70.8% compared with the Archie's formula (58%). The first two saturation methods are more reliable for shaly sand reservoir and they also match with earlier interpretations
Thus, average oil saturation of thick sand is found to be about 42%at depth interval 1531.8-1546m (TVD).
- Oil is also moveable within thick and thin sand reservoir of this formation. The estimated log derived average permeability from Wylie-Rose method has been estimated as 27.01 mD which is a good permeability for sand reservoir. So the oil pool of this formation is potential for production oil.

5.2 Recommendations:

- Hamra oil field is one of the onshore oil fields of the Sudan. From the current study of the available log data of this oil field, the following recommendations may be drawn:
- In order to assess the quality of the reservoir sand of variable thickness, whether it is thick or thin, and this field should be given careful attention in the light of formation evaluation with data from new drilled wells
- To estimate the water saturation of a reservoir, the special or routine core analysis is required. The estimated reservoir thickness, porosity and hydrocarbon saturation can be used for future reserve estimation and reservoir properties analysis of this formation.
- To assess the quality of the oil reservoir of Sudan accurately, special logging tools such as Nuclear Magnetic Resonance (NMR) and Formation Micro-Scanner (FMS) logs can be run with conventional wire line logs.

Reference:

- A .Y Mohammed , W .A.Ashcroft and A. J . Whiteman (2001) : Structural development and crustal stretching in the Muglad Basin , southern Sudan .
- Ali Sayed Mohammed Ibrahim . (2003) : Sedimentology and Reservoir Geology of the Middle-Upper Cretaceous Strata in Unity and Heglig Fields in SE Muglad Rift Basin ,Sudan .
- Avbovbo, J.A.,E.O.Ayoola ,and G.A.Osahon. (1986) : Depositional and structure styles northeastern Nigeria: AAPG Bulletin, v.70, p. 1787-1798
- Browne, S .E . and J. D. Fairhead. (1983) : Gravity study of the Central African rift system : a model of continental disruption ; 1, the Ngaoundere and Abu Gabra rift , P .Morgan , ed , Processes of continual rifting : Tectonophysics , v. 94, p. 187-203
- Fairhead, J.D., 1986 . Geophysical controls on sedimentation within the African rift systems . In : Frostlck , L.E., Renaut , R.W., Reid, I., Tlercehn, J.J.(Eds) Sedimentation in the African Rift : Geological Society Special Publication 25, pp. 19-22
- George Asquith with Charles Gibson . (1982) : Basic well log analysis for geologists .
- Girdler, JD ., Fairhead, R.C., Searle and W.T.C. Sowerbutts. (1969): Evolution of rifting in Africa : Nature, v.224, p. 1178-1182
- Mohamed , A.Y., Person, M. J., Ashcroft, W.A., Whiteman, A.J. (2002): Petroleum maturation modeling, AboGabra- Sharaf area , Mugade Basin, Sudan. Journal of African Earth Sciences 35, pp 331-344
- Mann, D.C., (1989). Thick-skin and thin-skin detachment faults in continental Sudanese rift basins. Journal African Earth Sciences 8, 307-322.
- Moniem, A., Yagoub , A., El Mustafa .A., Tayib.A, ELShaif . F., Mursi. H., Yousif.
- H., El Zein . L.A., Kehrer. P., Mamoon . A.R. (1984): Evaluation of petroleum wells .
- Program Released Within the Sudanese German Technical Cooperation (Unpublished Report) Geological and Mineral Resources Dept. (Sudan, 1984) .
- Mustafa, A.A, Tyson, R.V. (2002) : Organic Facies of Early Cretaceous synrift Lacustrine Source Rocks from the Mugled Basin, sudan .Journal of Petroleum Geology Vol.25 (3), July 2002, PP 351- 399..

Schull, T.J. (1988): Rift basin of interior Sudan: Petroleum exploration and discovery, AAPG Bull., 72, 1128-1142, Tulsa.

Robertson Research International Limited, (1990): The Petroleum Potential of Southern, Central and Eastern Sudan. Vol.2 Geological and Stratigraphical Framework (Unpublished report).

Wright, J.D.(1981): Review of origin and evaluation of the Benue trough in Nigeria: Earth Evolution Sciences, P. 98-103.

Ali Sayed Mohamed Ibrahim (2003) :investigated the depositional environment, source area and paleogeography of the early Cretaceous (Neocomian .Albian) strata of Sharaf and Abu Gabra formations 1 in the N-W. Muglad rift Basin of interior Sudan.

HananAbd El Mutaal Hussein (1997) :investigated in her study Cenomanian-Late Albian continental fluvial Bentiu formation based on data obtained from three exploration wells, in. W Muglad basin.

APPENDX

E-1 Estimation Lithology for MH -4Well :

| Number | Depth | ρ_p | ρ_{pcorr} | $\Phi\%$ |
|--------|--------|----------|----------------|----------|
| 1 | 1495.7 | 2.239 | 2.27 | 23.03 |
| 2 | 1497 | 2.107 | 2.14 | 30.9 |
| 3 | 1499 | 2.213 | 2.25 | 24.2 |
| 4 | 1501 | 2.134 | 2.13 | 31.5 |
| 5 | 1503.5 | 2.233 | 2.27 | 23.03 |

$$IGR = \frac{GR_{log} - GR_{min}}{GR_{max} - GR_{min}} = \frac{95 - 68.056}{136.5 - 68.056} = 0.39 \quad (5.1)$$

$$V_{sh} = 0.083 * (2^{3.7 * GR} - 1) = 0.083 * (2^{3.7 * 0.39} - 1) = 14.26\% \quad (5.2)$$

E-2 Assessment porosity from Density Log for MH-4 Well :

| Number | Depth | GRlog | IGR | Vsh% |
|--------|--------|-------|-------|-------|
| 1 | 1495.7 | 95 | 0.39 | 14.26 |
| 2 | 1497 | 94 | 0.37 | 13.1 |
| 3 | 1499 | 98 | 0.44 | 17.3 |
| 4 | 1501 | 73 | 0.073 | 1.6 |
| 5 | 1503.5 | 99 | 0.45 | 18 |

$$\rho_{pcorr} = \rho_p + V_{sh} * (\rho_{ma} - \rho_{cl}), \rho_{pcorr} = 2.239 + 0.1426 * (2.65 - 2.36) = 2.27 \quad (5.3)$$

$$\Phi = \frac{\rho_{ma} - \rho_p}{\rho_{ma} - \rho_{cl}} = \frac{2.65 - 2.27}{2.65 - 1} = 23.03\% \quad (5.4)$$

E-3 Assessment porosity from sonic Log for MH-4 Well :

| Number | Depth | ΔT_{Log} | ΔT_{max} | ΔT_f | Φ_e | Φ_e correct |
|--------|--------|------------------|------------------|--------------|----------|------------------|
| 1 | 1495.7 | 137 | 189 | 55 | 38% | 34.9 |
| 2 | 1497 | 131 | 189 | 55 | 43.3% | 38.9 |
| 3 | 1499 | 127 | 189 | 55 | 49.26% | 44.3 |
| 4 | 1501 | 141 | 189 | 55 | 35.8% | 32.2 |
| 5 | 1503.5 | 125 | 189 | 55 | 47.7% | 42.9 |

$$\Phi_e = \frac{\Delta T_{ma} - \Delta T_{Log}}{\Delta T_{ma} - \Delta T_f} = \frac{189 - 137}{189 - 55} = 38\% \quad (5.5)$$

$$\Phi_e \text{ correct} = 0.9 * \Phi \quad (5.6)$$

$$\Phi_e \text{ correct} = 0.9 * 38 = 34.9$$

(5.7)

E-4 Assessment porosity from Neutron Log for MH-4 Well:

| No | Depth | Vsh | ΦN | ΦN correct |
|----|--------|--------|------|------------|
| 1 | 1495.7 | 14.26% | 29.1 | 29 |
| 2 | 1497 | 13.1% | 16 | 15 |
| 3 | 1499 | 17.3% | 25.5 | 25.38 |
| 4 | 1501 | 1.6% | 19.2 | 19 |
| 5 | 1503.5 | 18% | 22.7 | 22.58 |

$$\Phi N \text{ correct} = \Phi N - (Vsh * 16) + 0. \quad (5.8)$$

$$\Phi N \text{ correct} = 29.1 - (14.26 * 16) + 0.04 = 2 \quad (5.9)$$

Example (1):

E-5 calculation RW and SW From SP Log for MH-2 Well :

Calculation of the Rw from Sp Log

There are many steps to determine the Rw:

- 1- Calculation formation temperature.
- 2- Estimation formation thickness
- 3- Correct SP to SSP from Log.
- 4- Determine the X value.
- 5- Calculate the $\frac{Rmf}{Rwe}$ ratio.
- 6- Calculate Rw from the correct (2) by using temperature and Rwe.

- Calculating steps :

TD = 1907 meter =6102.4ft.

- Bottom temperature = 72 °

F = 1.8 * C + 32 =161.6F

Rmf = 0.042

1-formation temperature@4901.76

The surface temperature = 28 c °

- $Y = mx + c$

$m \equiv$ slope

$$m = \frac{161.6 - 82}{6102.4} = 0.013$$

$$Y = 0.013 * 4901.76 + 61$$

$$Y = 146 \text{ F } ^\circ$$

Thickness = 45ft

- Correction to SSP :

Used curve (1)

$$\text{SSP} = S_p * \text{correct Factor}$$

$$\text{SSP} = 18 * 1.01 = 18.18$$

- $\text{SSP} = -K \text{Log} \frac{Rwfe}{Rwe}$

Calculate:

$$K = 61 + 0.133 * T_f$$

$$= 61 + 0.133 * 146 = 81$$

$$\frac{18.18}{81} = \frac{81}{81} = \text{Log} \frac{Rwfe}{Rwe}$$

$$0.226 = \text{Log} \frac{Rwfe}{Rwe}$$

$$1.68 = \frac{Rwfe}{Rwe}$$

$$Rwe = \frac{Rwfe}{1.43}$$

$$Rwfe = 0.85 * Rmf = 0.83 * 0.04712 = 0.04$$

$$Rwe = \frac{0.04}{1.43} = 0.023$$

By using curve (2) :

Calculate the $R_w = 0.04$

$R_t = 2.03$ Average zone

$$S_w = \sqrt{\frac{F * R_w}{R_t}}$$

$$F = \frac{1}{\Phi^m}$$

$$S_w = 0.41$$

$$S_o = 1 - S_w = 1 - 0.41 = 0.59$$

BVW = bulk volume water.

$$\Phi * S_w = 0.23 * 0.41 = 0.094$$

$$S_{xo} = (S_w)^{\frac{1}{s}}$$

$S_{xo} \equiv$ water saturation of unvirgen zone.

$S_w \equiv$ water saturation of unvirgen zone.

Moveable hydrocarbon Index :

$$\frac{S_w}{S_{xo}} = \left(\frac{\frac{R_{xo}}{R_t}}{\frac{R_{wf}}{R_w}} \right)^{\frac{1}{2}}$$

$R_{xo} \equiv$ Formation shallow resistivity.

$R_t \equiv$ Formation true resistivity.

$R_w =$ Resistivity water saturation.

$\frac{S_w}{S_{xo}} =$ moveable hydrocarbon.

$$S_{xo} = (S_w)^{\frac{1}{s}}$$

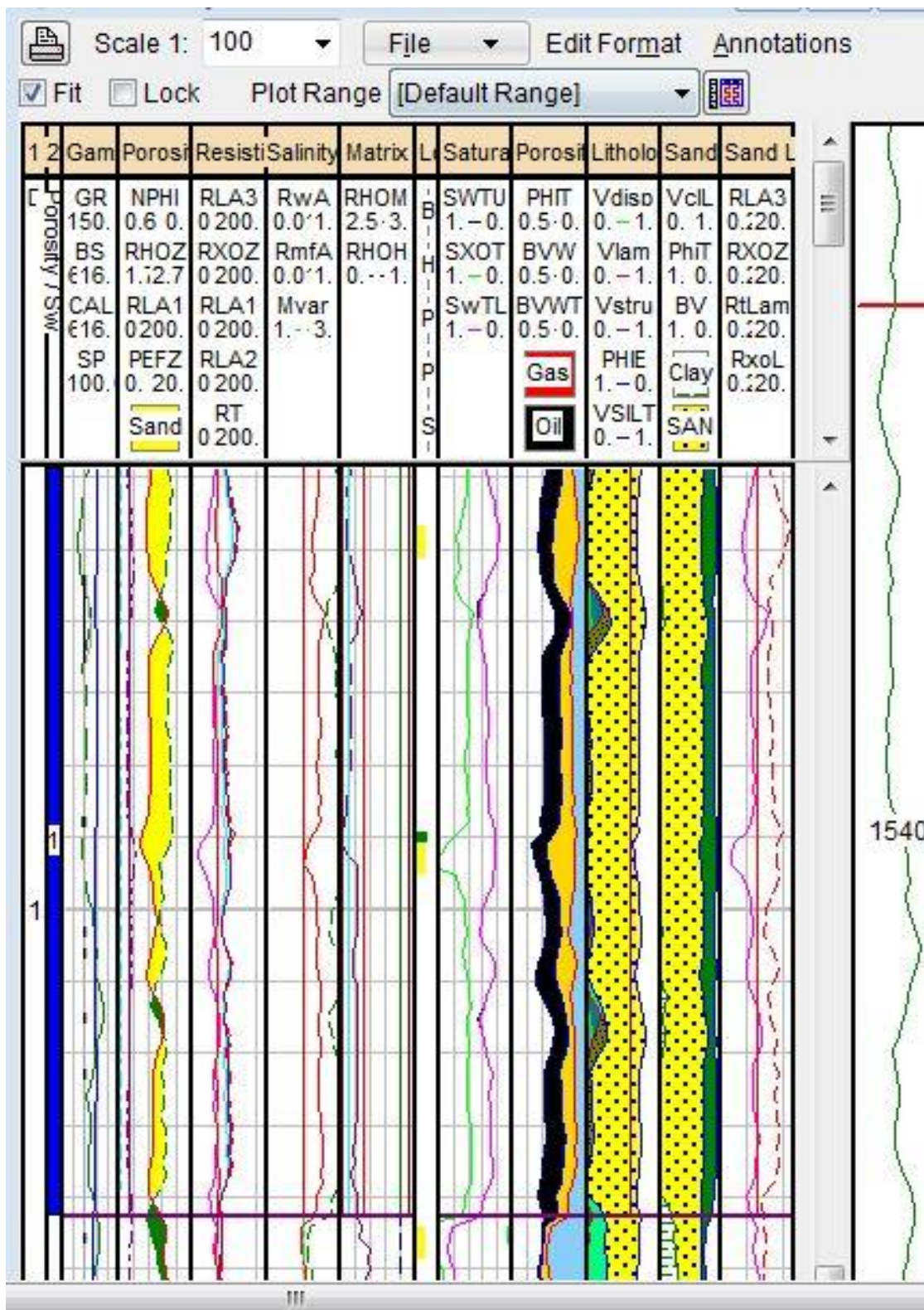
$$S_{xo} = (0.41)^{\frac{1}{5}} = 0.84$$

moveable hydrocarbon Index = 0.488

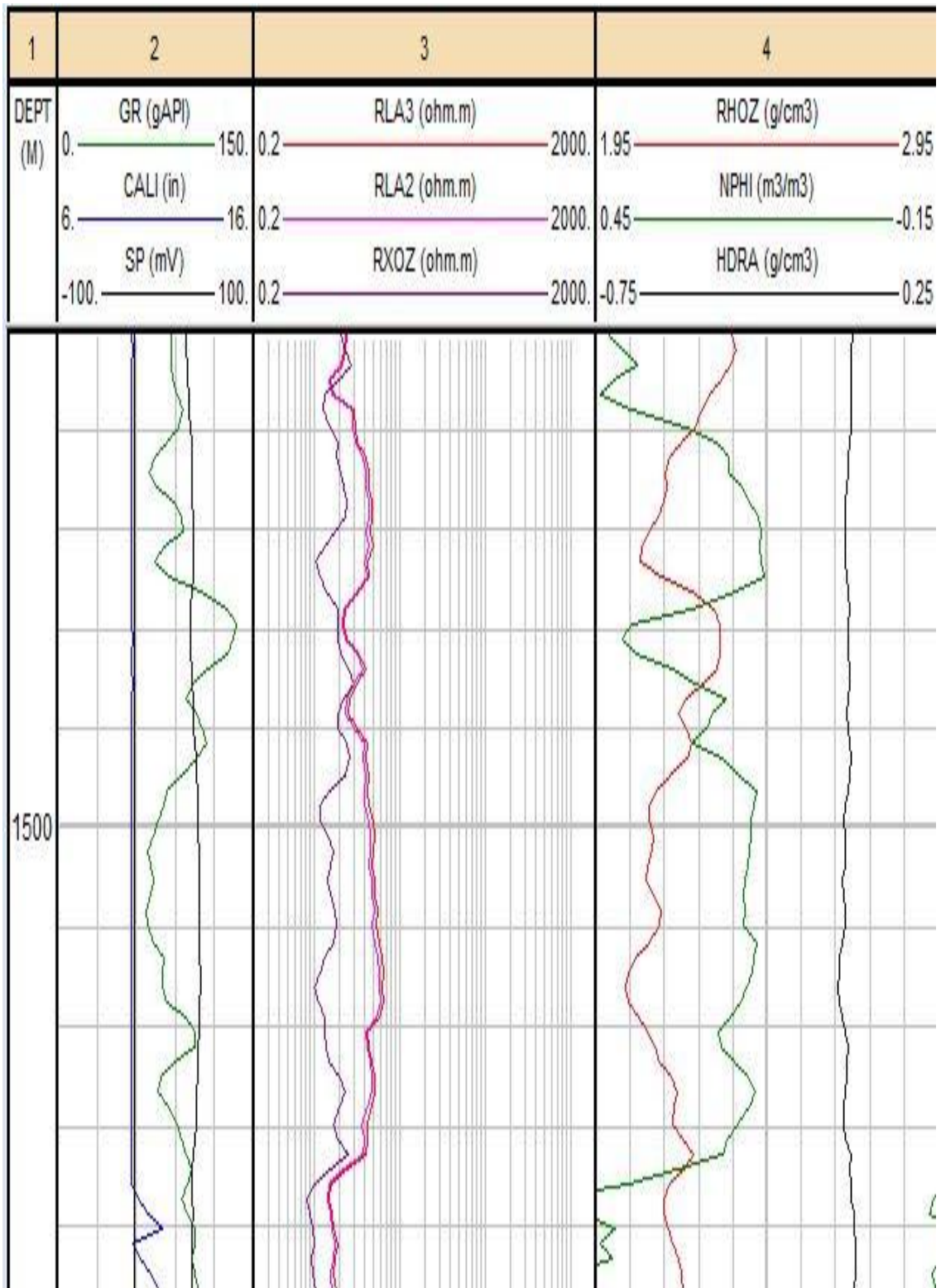
E-6 Table estimate petrophysical properties for MH-1

| Number | GRlog | Vsh% | | $Q_{p,corr}$ | $\Phi, s\%$ | Φ, N | $\Phi, N, c\%$ | Depth |
|--------|-------|-------|--------|--------------|-------------|-----------|----------------|--------|
| | | | Q_p | | | | | |
| 1 | 48 | 84.1 | 2.2893 | 2.53 | 7 | 0.296 | 16 | 1901.7 |
| 2 | 32 | 22.56 | 2.248 | 2.313 | 20.4 | 0.213 | 17.7 | 1909 |
| 3 | 13 | 1.16 | 2.252 | 2.255 | 23.9 | 0.177 | 17.55 | 1918 |
| 4 | 16 | 3 | 2.3 | 2.3 | 15.93 | 0.215 | 12.5 | 1925 |
| 5 | 46 | 74.6 | 2.33 | 2.552 | 5.9 | 0.213 | 19.37 | 1932 |

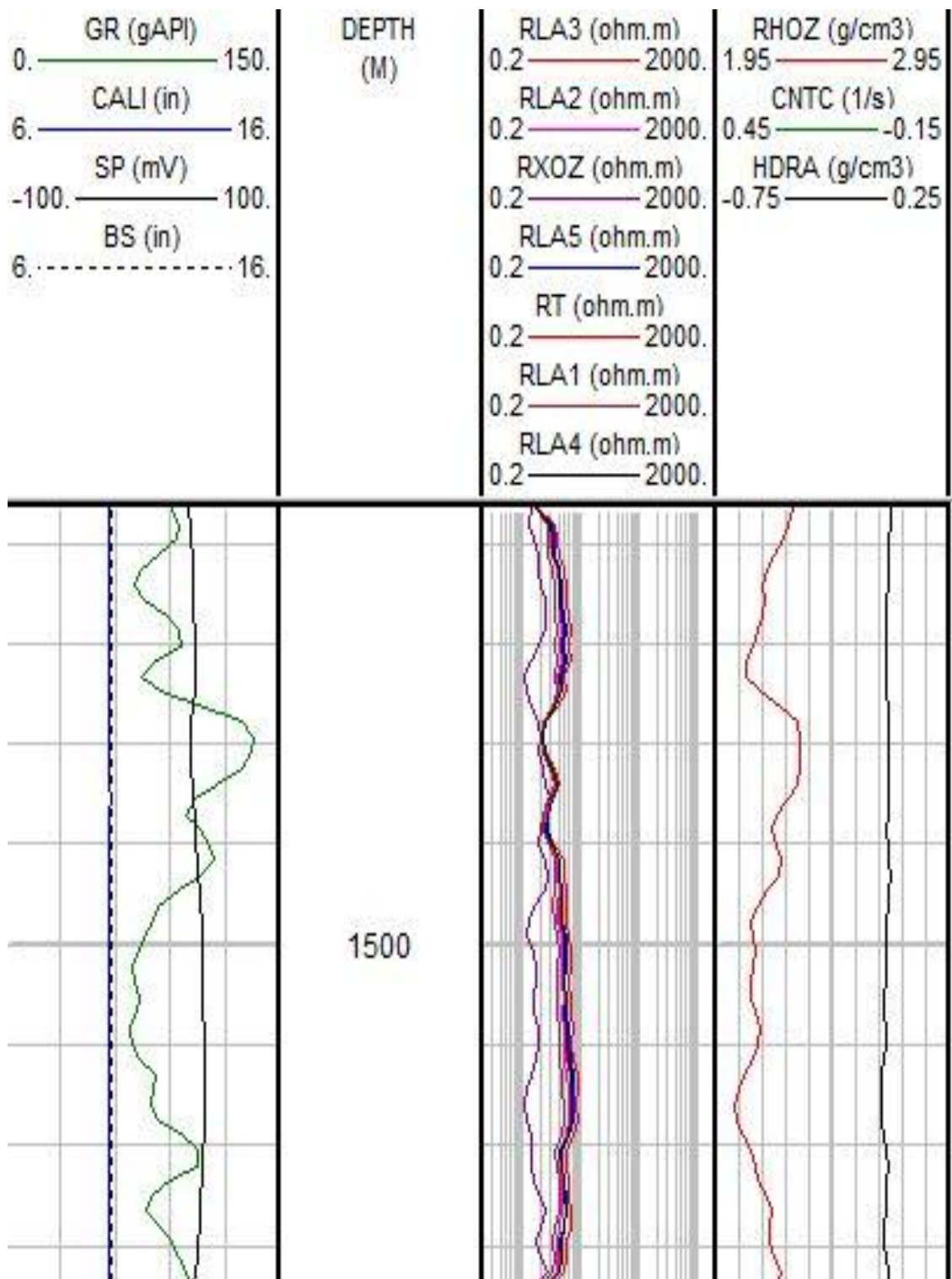
- RW=0.032
- Sw=0.2
- So=0.8
- BVW=0.032



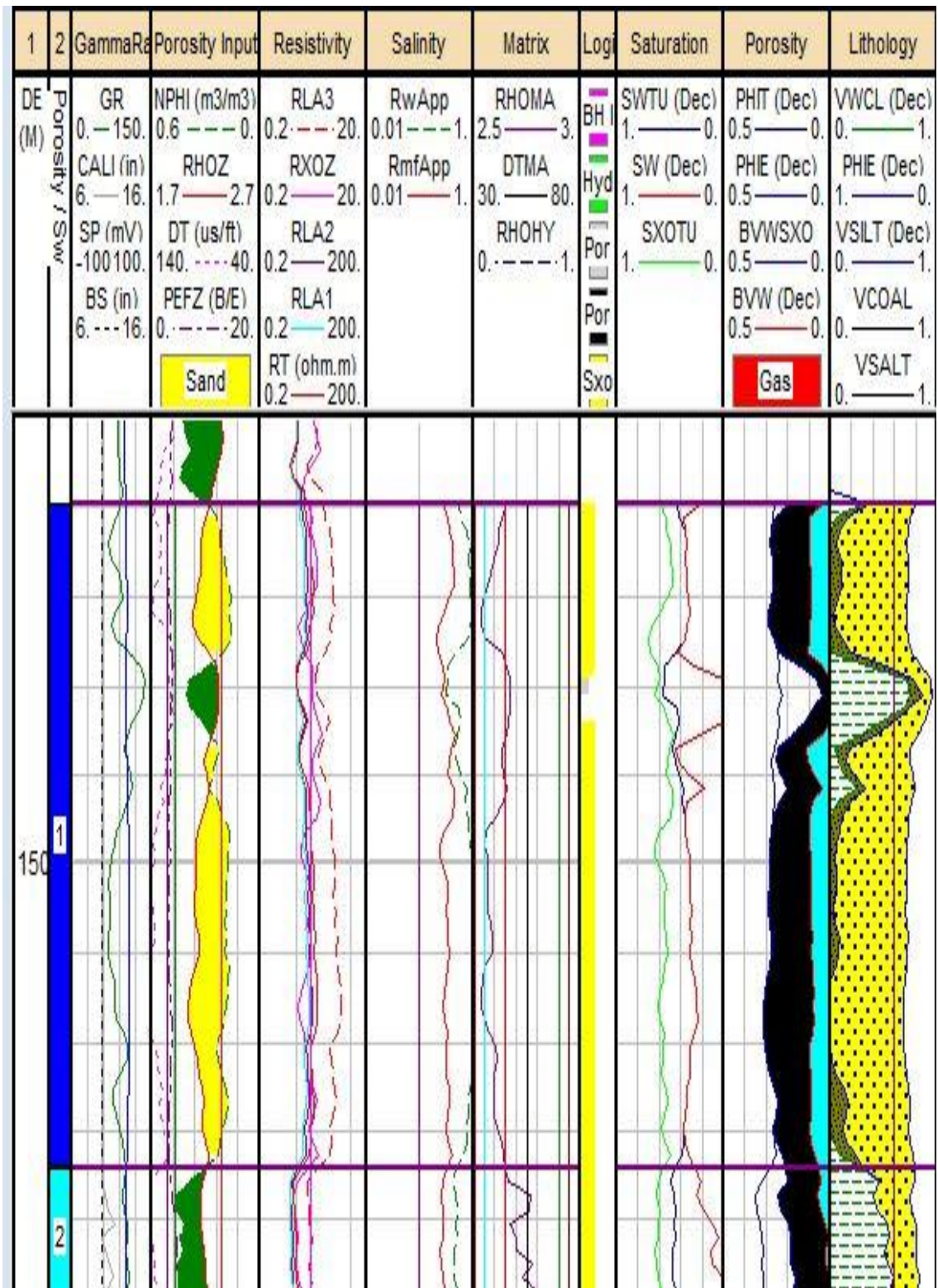
Appendix-A1 -Lithology and Resistivity logs and saturation layers MH-2



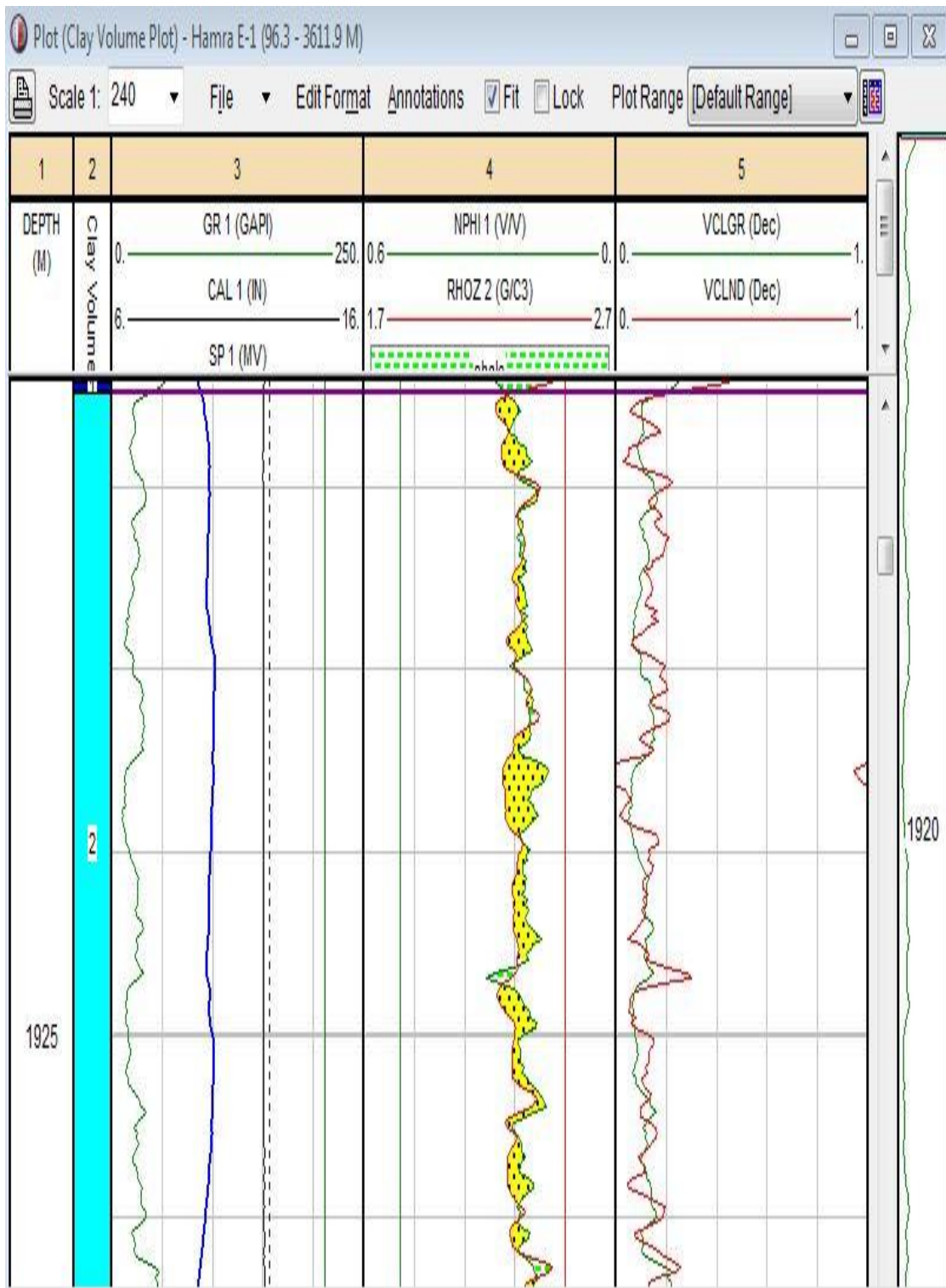
Appendix-A2 -Lithology and Resistivity logs and Spectral density, Dual spaced neutron MH-2



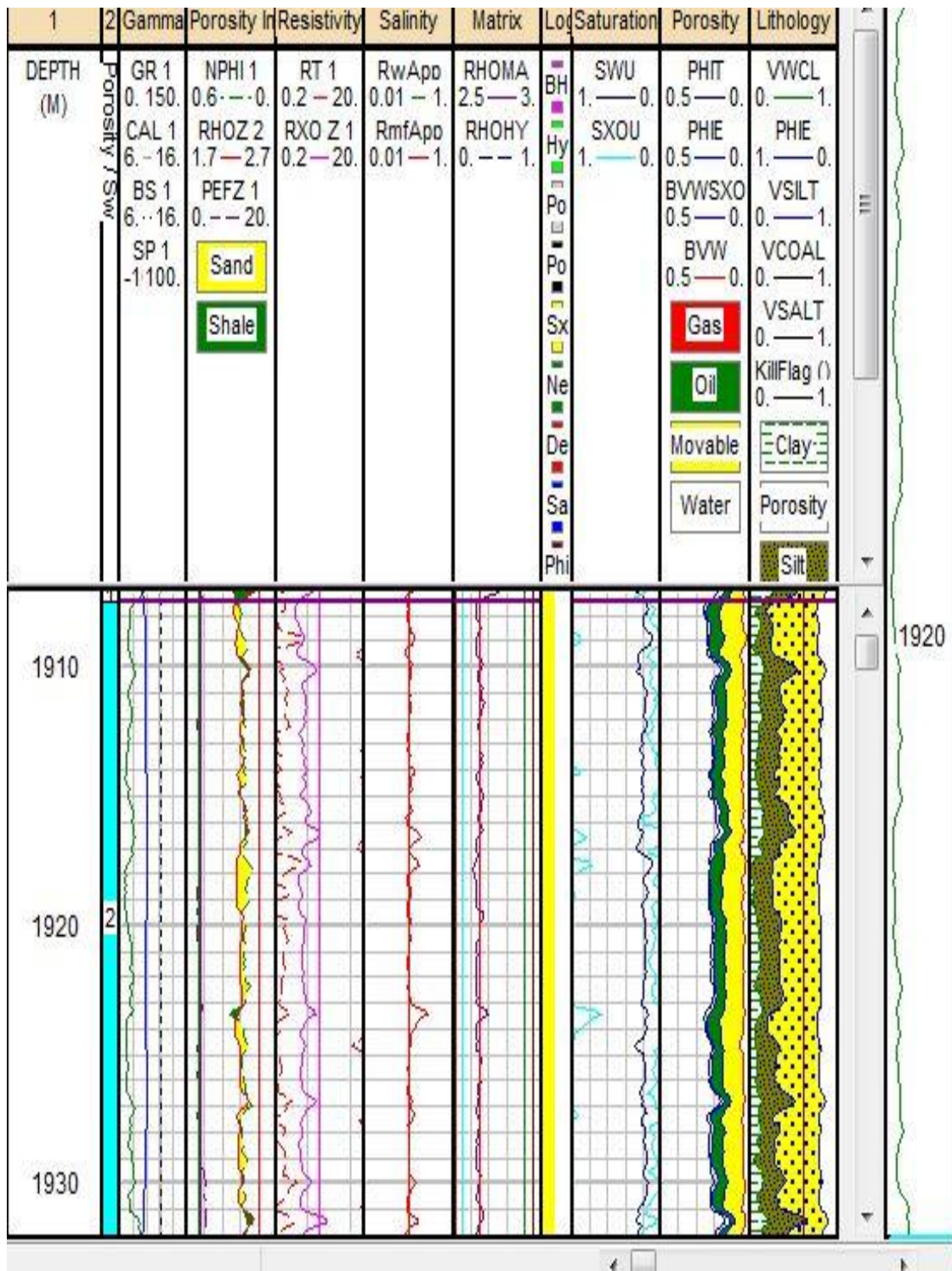
Appendix-A 3 -Lithology and Resistivity logs vsh MH-4



Appendix-A4 -Lithology and Resistivity logs and saturation layers



Appendix-A5 -Lithology and Resistivity logs and Spectral density, Dual spaced neutron MH-1

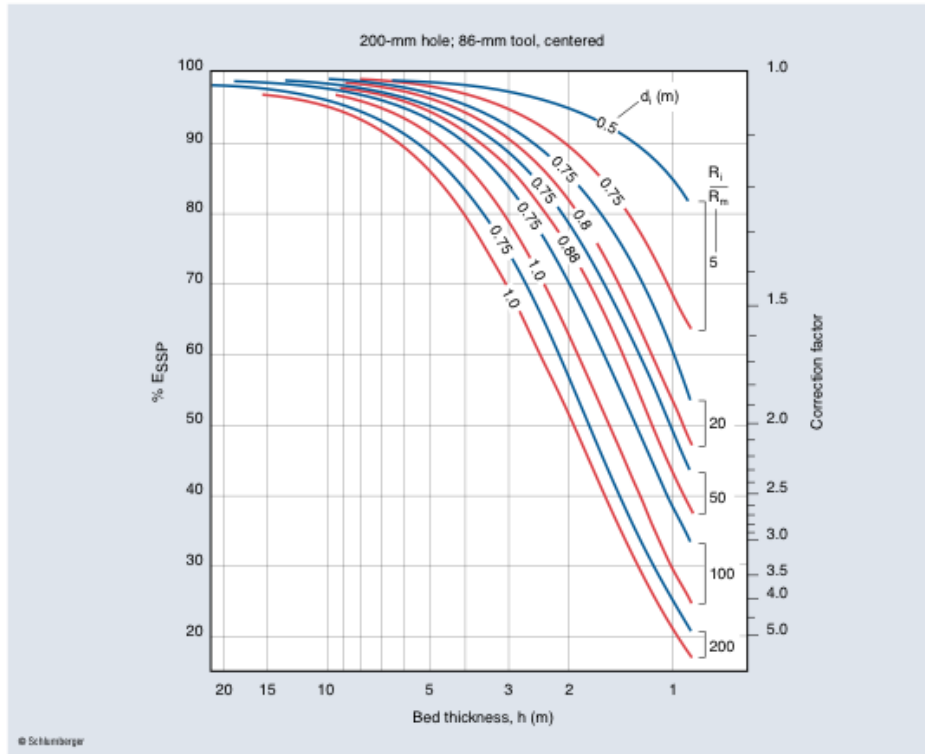


Appendix-A6 -Lithology and Resistivity logs and Spectral density, Dual spaced neutron MH-1

SP Correction Chart (Empirical)

SP-4m
(Metric)

SP



Example: SP = -80 mV in a 3-m bed
 $R_m = 0.5$ ohm-m, and R_i (invaded zone resistivity) =
 10 ohm-m (both at formation temperature)
 Invasion diameter = 0.80 m

Therefore, $R_i/R_m = 10/0.5 = 20$
 SP correction factor = 1.1
 Corrected SP, $E_{SSP} = -80 (1.1) = -88$ mV

